26. Clements JA, Matheson BA, Wines DR, Brady JM, MacDonald RJ, Funder JW (1988) Androgen dependence of specific kallikrein gene family members expressed in rat prostate. *J Biol Chem* 263: 16132–16137.
27. Onozawa M, Fukuda K, Watanabe M, Ohtani M, Akaza H, Sugimura T, Wakabayashi K (2001) Detection and cloning of a protein recognized by anti-human prostate-specific antigen (PSA) antibody in the rat ventral prostate. *Jpn J Cancer Res* 92: 863–868.
28. Byrne RL, Leung H, Neal DE (1996) Peptide growth factors in the prostate as mediators of stromal epithelial interaction. *Br J Urol* 77: 627–633.
29. Nishi N, Oya H, Matsumoto K, Nakamura T, Miyanaka H, Wada F (1996) Changes in gene expression of growth factors and their receptors during castration-induced involution and androgen-induced regrowth of rat prostates. *Prostate* 28: 139–152.
30. Torring N, Jorgensen PE, Poulsen SS, Nexo E (1998) Epidermal growth factor in the rat prostate: production, tissue content and molecular forms in the different prostatic lobes. *Prostate* 35: 35–42.
31. Marengo SR, Chung LW (1994) An orthotopic model for the study of growth factors in the ventral prostate of the rat: effects of epidermal growth factor and basic fibroblast growth factor. *J Androl* 15: 277–286.
32. Zhu N, Pewitt EB, Cai X, Cohn EB, Lang S, Chen R, Wang Z (1998) Calreticulin: an intracellular Ca++-binding protein abundantly expressed and regulated by androgen in prostatic epithelial cells. *Endocrinology* 139: 4337–4344.
33. Jiang F, Yang L, Cai X, Cyriac J, Shechter I, Wang Z (2001) Farnesyl diphosphate synthase is abundantly expressed and regulated by androgen in rat prostatic epithelial cells. *J Steroid Biochem Mol Biol* 78: 123–130.
34. Weihua Z, Makela S, Andersson LC, Salmi S, Saji S, Webster JI, Jensen EV, Nilsson S, Warner M, Gustafsson JA (2001) A role for estrogen receptor beta in the regulation of growth of the ventral prostate. *Proc Natl Acad Sci USA* 98: 6330–6335.
35. Horvath LG, Henshall SM, Lee CS, Head DR, Quinn DI, Makela S, Delprado W, Golovsky D, Brenner PC, O'Neill G, Kooner R, Stricker PD, Grygiel JJ, Gustafsson JA, Sutherland RL (2001) Frequent loss of estrogen receptor-beta expression in prostate cancer. *Cancer Res* 61: 5331–5335.
36. Banerjee PP, Banerjee S, Tilly KI, Tilly JL, Brown TR, Zirkin BR (1995) Lobe-specific apoptotic cell death in rat prostate after androgen ablation by castration. *Endocrinology* 136: 4368–4376.
37. Zhang J, Thomas TZ, Kasper S, Matusik RJ (2000) A small composite probasin promoter confers high levels of prostate-specific gene expression through regulation by androgens and glucocorticoids in vitro and in vivo. *Endocrinology* 141: 4698–4710.
38. Gubits RM, Shaw PA, Gresik EW, Onetti-Muda A, Barka T (1986) Epidermal growth factor gene expression is regulated differently in mouse kidney and submandibular gland. *Endocrinology* 119: 1382–1387.
39. Fujimoto N, Asano K, Usui T, Honda H, Kitamura S (2005) Cloning and characterization of the 5'-flanking region of the rat estrogen receptor beta gene. *J Steroid Biochem Mol Biol* 94: 15–21.
40. Claessens F, Rushmere NK, Davies P, Celis L, Peeters B, Rombauts WA (1990) Sequence-specific binding of androgen-receptor complexes to prostatic binding protein genes. *Mol Cell Endocrinol* 74: 203–212.

Available online at www.sciencedirect.com
ScienceDirect
Journal of Steroid Biochemistry & Molecular Biology 105 (2007) 57–62
The Journal of Steroid Biochemistry & Molecular Biology
www.elsevier.com/locate/jsbmb

In vivo function of the 5′ flanking region of mouse estrogen receptor β gene

Nariaki Fujimoto [a,*], Osamu Nakajima [b], Shigeyuki Kitamura [c], Shigeru Ohta [c]

[a] *Department of Developmental Biology, Research Institute for Radiation Biology and Medicine (RIRBM), Hiroshima University, 1-2-3 Kasumi, Minami-ku, Hiroshima 734-8553, Japan*
[b] *Research Laboratory for Molecular Genetics, Yamagata University, Yamagata 990-9585, Japan*
[c] *Department of Xenobiotic Metabolism and Molecular Toxicology, Institute of Pharmaceutical Sciences, Hiroshima University School of Medicine, Kasumi 1-2-3, Minami-ku, Hiroshima 734-8551, Japan*

Received 14 August 2006; accepted 21 December 2006

Abstract

The estrogen receptor (ER) subtypes α and β differentially distributed in tissues, and ERβ is present preferentially in epididymis, testis, prostate, ovary and lung. Although transcription promoter activity has been found in the 5′ flanking (5′f) region of the ERβ gene, it is not known whether the proximal 5′f region is responsible for the tissue-specific distribution. In the present study, we examined the *in vivo* promoter activity of this region in transgenic mice with the lacZ reporter. About 2.2 kbp of the proximal 5′f region of ERβ was cloned and inserted into reporter plasmids. This 5′f region of mouse ERβ, which displayed a substantial promoter activity *in vitro*, was very similar to that in rats, but showed limited homology with the human gene. Three independent lines of mice containing ERβ-5′f-lacZ were obtained. Quantitative measurement of mRNA showed that lacZ was expressed only in the testis, in which sertoli cells as well as a part of the spermatogonia were confirmed to be lacZ-positive, in accordance with the known localization of ERβ expression in the testis. The present study suggests that a 2.2 kbp of the 5′f region of the ERβ gene is able to direct testis-specific expression, but is not itself sufficient to determine the expression in other organs.

Keywords: Estrogen receptor beta; Promoter; Transgenic mouse; *In vivo* analysis

1. Introduction

Estrogen-dependent biological function is mediated by two subtypes of estrogen receptor (ER), α and β [1]. ERα mediates classical estrogen responses, such as uterine growth and mammary gland development. In addition, ERα function is essential for sperm fertilization in the testis [2,3]. ERβ, on the other hand, is necessary to maintain a normal ovulation frequency in the ovary and plays anti-proliferative roles in the prostate and mammary glands. While significant amounts of ERα are present in a variety of sites, including bone, liver and skeletal muscle, as well as reproductive tissues, ERβ distribution seems more limited, with significant expression only in thymus, testis, prostate and ovary. Previous studies have indicated that transcription of the ERα gene is determined by multiple untranslated first exons and promoters [4–6]. Six untranslated first exons have been identified in the human case and four in the rat and the mouse [7–9]. The transcripts are generated by differential promoter usage and differ in the 5′ untranslated exon 1 because of alternative splicing events. In addition, intronic promoter activity was recently found to be involved in the transcription of variant ERα [10]. In the case of ERβ, two isoforms of human ERβ mRNA containing different untranslated 5′-ends have been reported, suggesting the existence of two distinct promoter structures for the gene [11,12]. On the other hand, our previous study and others have demonstrated that rat and mouse ERβ mRNA has a single end structure [13,14]. About 0.7 kbp of the 5′ flanking (5′f) region of ERβ was determined in both

* Corresponding author. Tel.: +81 82 257 5820; fax: +81 82 256 7107.
E-mail address: nfjm@hiroshima-u.ac.jp (N. Fujimoto).

0960-0760/$ – see front matter © 2007 Elsevier Ltd. All rights reserved.
doi:10.1016/j.jsbmb.2006.12.103

species and found to be highly homologous. *In vitro* reporter gene analysis demonstrated that the region determines basic as well as cell-specific transcriptional activity in both species.

Although *in vitro* studies have suggested that the 5′f region of ERβ gene may be involved in tissue-specific distribution of ERβ, the question of whether it is sufficient for *in vivo* transcriptional regulation has yet to be addressed. In the present study, therefore, promoter activity of the 5′f region of ERβ gene was examined *in vivo*. The 2.2 kbp region from the transcription starting site was cloned and connected into a lacZ reporter gene to create transgenic mice. The reporter expression was determined by quantitative RT-PCR, as well as lacZ staining, in individual tissues.

2. Materials and methods

2.1. Animals

Animal experiments were conducted according to the guidelines of the Guide for the Care and Use of Laboratory Animals of Hiroshima University and The Animal Welfare Regulations of Yamagata University School of Medicine. BDF1 mice were obtained from CLEA Japan Inc. (Tokyo, Japan) and maintained under constant conditions with free access to basal diet and tap water. Animals were sacrificed under anesthesia and tissues were dissected out, and immediately fixed in RNA Later solution (Ambion, Inc., Austin, TX, USA) for RNA extraction. Portions of the tissues were fixed in 2% formaldehyde/0.2% glutalaldehyde fixation solution, incubated in 20% sucrose solution and embedded in OTC compound (Miles Inc., Elkhart, Indiana, USA) for frozen sectioning.

2.2. Cell culture

The rat prostate cell line, DT3, was maintained in DME medium (Sigma Chemical Co., St. Louis, MO, USA) containing penicillin and streptomycin with 5% FBS (Gibco/Invitrogen Corp., Carlsbad, CA, USA). For hormone treatment, cells were maintained for a week in phenol red-free medium (Sigma Chemicals) containing the same antibiotics along with dextran-charcoal treated sera.

2.3. Genomic DNA library screening

To isolate a genomic 5′f region of ERβ exon 1, a 129SVJ library in λFIX II (Stratagene, La Jolla, CA, USA) was screened with a 809-bp cDNA probe containing the previously reported exon 1 and 5′f region of mERβ (Genbank accession AB034985). Two clones were purified and sequenced to the transcriptional starting site with an ABI model 310 sequencer (PerkinElmer Life Sciences, Boston, MA, USA).

2.4. Construction of luciferase reporter plasmids and transient transfection

Truncated fragments of the 5′f region of mouse ERβ were prepared by accurate PCR with LA-Taq (Takara Bio Inc., Ohtsu, Japan) between −2145, −1343, −692, −149, −60 and +193 (relative to the transcriptional starting site) from the cloned fragment. Each was cloned into PCR2.1-TOPO vector (Invitrogen) and then SacI/XhoI fragments were inserted into the same restriction enzyme site of the pGL_3-basic luciferase reporter plasmid (Promega Co., Madison, WI, USA). phRL-CMV (Promega) was employed as an internal control. DT3 cells were plated at 2×10^4 per well in 48-well plates and transiently transfected with 300 ng of a reporter and 5 ng of phRL-CMV with TransFast transfection reagent (Promega). The weight ratio of TransFast reagent to DNA was 1:1. After 24 h incubation, cells were harvested with 30 μl of cell lysis buffer (Promega) and the firefly and renilla luciferase activities were determined with a Dual Luciferase Assay Kit (Promega) by measuring luminescence with a Wallac Micro-Beta Scintillation Counter (PerkinElmer Life Sciences). Firefly luciferase reporter activity was normalized to renilla luciferase activity from phRL-CMV.

2.5. Construction of lacZ reporter transgene and generation of transgenic mice

A pUC18-based reporter plasmid, placF, containing a nuclear localization signal (nls), lacZ, and mouse protamine polyA was a gift from Richard Palmiter at the University of Washington, Seattle, WA, USA [15]. A 2.3-kb fragment of the 5′f region of mouse ERβ (−2145 to +193, relative to the transcriptional starting site) was cut out from the pCR2.1-TOPO vector and inserted into placF. KpnI/HindIII digestion gave a 6.2 kb fragment of ERβ 5′f connected to nls-lacZ-poly(A). The construct was microinjected into the pronuclei of single-cell fertilized mouse embryos to generate transgenic mice, as previously described [16,17]. To detect the exogenous lacZ gene, genomic DNA was extracted from the tail tissues of pups, and PCR was performed with one primer specific for the ERβ 5′f region and another primer specific for lacZ.

2.6. Quantification of mRNA by real-time RT-PCR

Details were as described previously [18]. Total RNA was isolated from tissue and reverse-transcribed. A QuantiTect Sybr Green PCR kit (Qiagen) and an ABI Prism 7700 (Perkin-Elmer Co.) were employed for quantification of cDNA according to the supplied protocol. The following specific forward and reverse PCR primers with a Tm of about 59 °C were designed: 5′-CGATCTTCCTGAGGCCGATAC and 5′-TGTGAGCGAGTAACAACCCGT for lacZ (+231 to +381, 151 bp) and 5′-TCTGGACACCTCTCTCCTTT and 5′-CAACCGCTCCCGCCAAGCTT for mouse ERβ (+112 to +263, 152 bp) and 5′-CTGTCCCTGTATGCCTCTGGTC and 5′-TGAGGTAGTCCGTCAGGTCCC for mouse β-actin

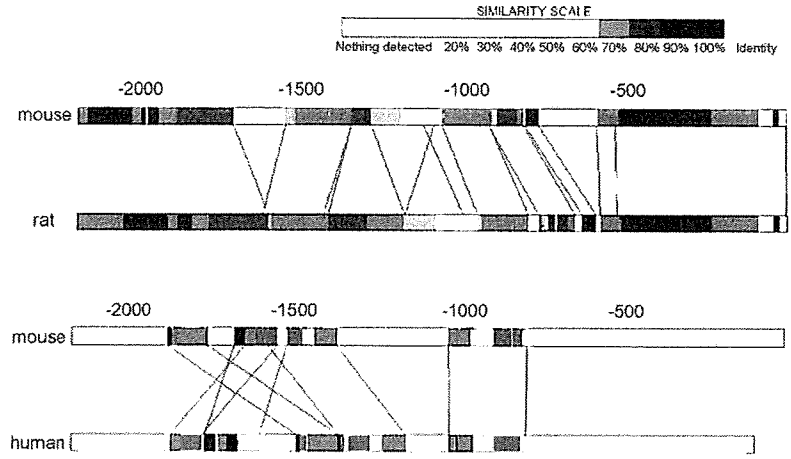

Fig. 1. Sequence comparison of the 5′f regions of mouse, rat and human ERβ. The sequences of 2.2 kbp of the 5′f region of mouse and rat ERβ (DQ273590 and DQ273589) and the corresponding human region (AF191544) were compared by using LFasta (Pôle Bioinformatique Lyonnais).

(+340 to +490, 151 bp). Measured mRNA contents were normalized with reference to β-actin mRNA.

2.7. Quantification of the transgene copy number

The gene copy number of lacZ was also determined with the real-time PCR based method described by Kindich et al. [19]. The genomic DNAs from tails were subject to real-time PCR analysis. The same primer set above was used for the determination of lacZ gene. Androgen receptor gene, a single copy gene in male animals, was employed as a reference. The PCR primers were 5′-CACCATGCAACTTCTTCAGCA (504–524) and 5′-TGAATTGCCCCCTAGGTAACT (+565 to +730 in exon 1, 191 bp).

2.8. Histochemical analysis of lacZ expression in mouse tissues

Sections (40 μm thick) from frozen tissues embedded in OCT compound were mounted onto microscope slides. They were fixed in 0.2% glutalaldehyde in PBS and incubated in PBS containing 1 mg/ml X-gal, 5 mM $K_4Fe(CN)_6$, 5 mM $K_3Fe(CN)_6$ and 2 mM $MgCl_2$. The reaction was stopped by washing with PBS and the sections were counterstained with 1% eosin, dehydrated in alcohol, treated with xylene, and mounted in Eukitt (O. Kindler GmbH, Freiburg, Germany).

2.9. Statistical analysis

Statistical comparisons were made using Student's *t*-test.

3. Results

3.1. Genomic structure of the 5′ flanking region of mouse ERβ

Two lamda phage DNAs containing a 5′f region of mouse ERβ were obtained from the 129SVJ mouse genomic library. A 2827 bp region from the transcription starting site was sequenced (GenBank accession DQ273590) and compared with the 5′f regions of rat ERβ (DQ273589) and human ERβ (AF191544) by use of the Local Alignment Tool, LFasta, at Pôle Bioinformatique Lyonnais (http://www.pbil.univ-lyon1.fr/pbil.html). High homology is evident between mouse and rat (70–90% similarity throughout the region), but there is only a limited sequence homology of the rodent and human ERβ promoter regions (Fig. 1). Motif analysis (http://www.motif.genome.jp/) showed the 5′f region to contain the consensus promoter motifs AML-1a, SRY, GATA-3 and cdxA (Fig. 2A).

3.2. In vitro promoter activity of mERβ-5′f

The results of examination of the promoter activity of the cloned 5′f region and some of the deletion fragments of mERβ are summarized in Fig. 2B. The luciferase activity of ERβ-5′f (2145/+193)-luc was similar to those of the truncated reporters −1343/+193, −692/+193 and −149/+193, while no activity was seen with −60/+193.

3.3. Generation of mERβ-5′f-lacZ-transgenic mice and lacZ mRNA levels in different tissues at 10 weeks of age

After microinjection and embryo implantation, three lines of transgenic mice (lines 420, 481 and 561) were successfully established. No neonatal or adult deaths were observed in mERβ-5′f-lacZ mice. Quantitative PCR of lacZ in genomic DNA showed that the numbers of transgene copies were 2, 5–6, and 4 per genome in lines 420, 481 and 561, respectively. Table 1 shows the lacZ and ERβ mRNA levels in several tissues of each line of F1 mice at 10 weeks of age. While high ERβ mRNA levels were evident in the epididymis, lung, ventral prostate, testis and ovary, significant lacZ mRNA expression was noted only in testis, although the levels differed among the transgenic mouse lines. In lines 481 and

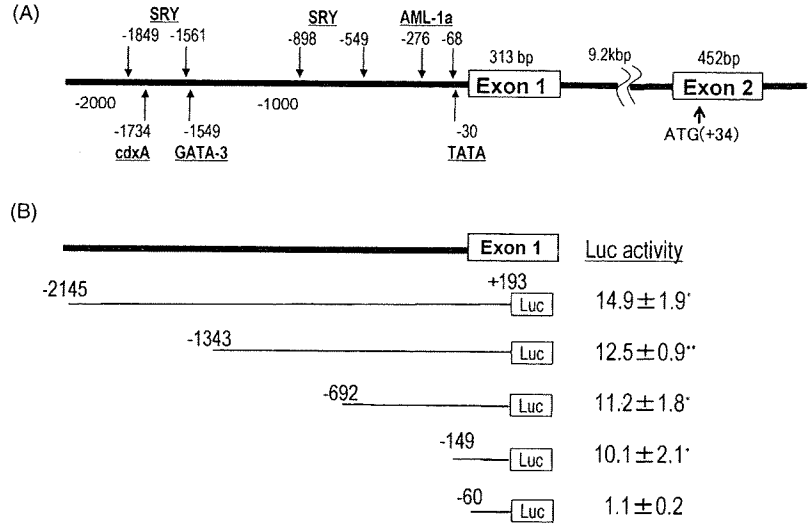

Fig. 2. (A) Structure of the 5′f region of mouse ERβ. Arrows indicate putative *cis*-acting motifs (only consensus motifs are displayed). Numbers indicate positions relative to the transcription starting site (exon 1). (B) Successive 5′-deletion analysis of mouse ERβ promoter activity. Luciferase reporters containing fragments of 5′ flanking regions of ERβ were transiently transfected into an ERβ-positive rat prostate cancer cell line DT3. Values are relative to that with the null-luc-reporter (mean ± S.E.M., $n = 3$).

Table 1
LacZ and ERβ mRNA in mERβ-5′f-lacZ-TG mice

	Ovary	Epididymis	Lung	Ventral prostate	Testis	Liver	Thym	Kidney	Spleen
LacZ									
Line 420	–	0.2	0.5	0.0	238	0.2	n.d.	n.d.	n.d.
Line 481	0.25	35.5	4.9	4.3	1329	5.9	2.1	3	3.5
Line 561	0.16	28.5	15.5	1.4	890	3.8	0.9	0.4	0.4
ERβ									
wt	20.0	9.2	3.2	1.9	0.4	0.0	0.1	0.0	0.0

Values are mRNA levels divided by β-actin mRNA levels (mol/mol β-actin). Eleven-week-old F1 mERβ-5f-lacZ-transgenic mice were sacrificed. Total RNA was isolated from tissues and lacZ mRNA levels were measured by real-time PCR. The numbers of transgene copies were 2, 5–6, and 4 per genome in lines 420, 481 and 561, respectively.

561, lacZ mRNA expression in the epididymis was higher than that in clearly negative tissues.

3.4. *LacZ straining in mERβ-5′f-lacZ-transgenic mice*

LacZ activity was detected in *in situ* frozen tissue sections of epididymis, lung, ventral prostate, testis, ovary and liver in 10-week-old F1 transgenic mice. Positive staining was observed only in the testis (Fig. 3). Localization of staining in the outer line of seminiferous tubules, as well as the triangular shape of the stained cells, suggested that the stained cells were sertoli cells. In addition, a part of the spermatogonia may be lacZ-positive. The partial staining of Leydig cells is probably artifact, since it was also observed in the wild-type testis.

4. Discussion

The 5′f region of the ERβ gene has been cloned and proved to have promoter activity in mice as well as humans in cell culture studies [14,12]. A region containing 692 bp from the transcription start site of mouse ERβ was sequenced and found to contain several putative *cis*-acting elements. Successive 5′-deletion analysis with luciferase reporters suggested that the promoter for basal transcriptional activity was located near the transcriptional start site, while the other elements may contribute to modulating the transcription. Our cloning and *in vitro* promoter analysis of the 5′f region of rat ERβ gave very similar results [13]. In the present study, the region of the mouse ERβ gene extending to −2139 bp was further cloned and luciferase reporter assay was carried out in a prostate cell line, DT3. The results were in line with those of previous reports, since the reporters containing 2.1, 1.3, 0.7 and 0.15 kbp of the 5′f region of mERβ showed similar transcriptional activity, while a −60 bp reporter showed no activity. Comparison of the 5′f regions revealed a high degree of similarity between the mouse and rat sequences, while the human sequence shows only partial homology with those of rodents and contains different *cis*-acting elements (AML-1a, Nkx-2.5 and AP-1). Recently, a second isoform of human ERβ mRNA containing different untranslated 5′-ends was

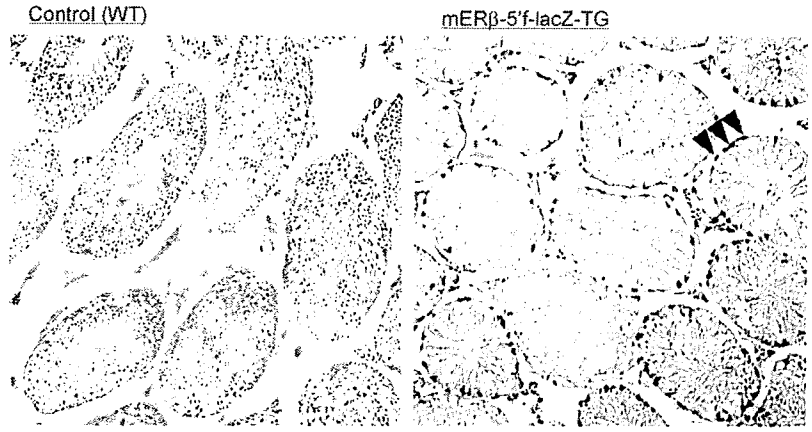

Fig. 3. LacZ staining in testis in WT and ERβ-5′f-TG mice. Sertoli cells as well as a part of the spermatogonia are lacZ-positive (arrowheads). Staining of Leydig cells is an artifact (also present in control).

reported to be specifically expressed in ejaculated spermatozoa and peripheral leukocytes, indicating the existence of two distinct promoter structures for the human ERβ gene [11].

Significant amounts of ERα are present in a variety of sites including pituitary, bone, liver and skeletal muscle, as well as reproductive tissues, such as ovary, uterus and mammary gland, while ERβ expression is restricted mainly to lung, thymus, testis, epididymis, prostate and ovary [1,20,21]. In addition, the tissue distribution of ERβ seems differ among species [22,23]. In humans, higher levels of ERβ mRNA were detected in the thymus, testis and ovary, while the prostate is the major ERβ-positive tissue in rats. On the other hand, in mice, ERβ mRNA is expressed in the epididymis, testis, prostate, ovary and lung. Previous *in vitro* studies have showed that the 5′f region of ERβ is responsible for cell-specific expression, i.e., higher luciferase reporter activities were noted in ERβ-positive cell lines than in ERβ-negative lines [13,14,12]. However, *in vivo* functional analysis remains necessary to determine whether the identified promoter regions control the tissue-specific ERβ expression.

In the present study, we successfully generated transgenic mice containing a mERβ-5′f-lacZ reporter. Three lines were obtained and showed similar tissue distribution patterns of lacZ mRNA expression, which suggested that the expression results from the transgene itself, not from specific insertion sites of the transgene. Data clearly demonstrated a testis-specific expression of lacZ, though a low level of lacZ expression may be present in the epididymis. The differences of mRNA levels among the lines seem to depend on the number of copies of the transgene. In testis, expression of lacZ was localized in sertoli cells, as well as a part of the spermatogonia, in agreement with previous findings based on immunostaining of ERβ expression in the mouse testis [24]. Sertoli cell-specific expression of ERβ has been confirmed by immunostaining, as well by *in situ* hybridization, in rat testis [25,26]. In addition, a recent investigation suggested that 17β-estradiol and 5α-androstane-3β (3β-diol), a possible physiological ERβ ligand converted from 5α-dihydrotestosterone in the tissue, may modulate sertoli cell function through ERβ [27]. Although expression of ERβ in sertoli cells of the testis is evident in rats as well as mice, it remains controversial whether it is expressed in human testis [28].

ERα expression is regulated by multiple untranslated first exons and promoters. At least four promoters have been postulated for the mouse ERα gene [5,8]. Two proximal promoters, called A and B, are responsible for the expression in most ERα-positive organs, including mammary gland, uterus and ovary, while the other two distal promoters seem to determine liver- and testis-specific expression. An *in vivo* functional analysis of the 5′f region of mouse ERα gene using transgenic mice demonstrated that a proximal 5′f region (promoter A) is sufficient for expression in a variety of organs, including mammary gland and uterus [29]. In contrast, our results indicate that the promoter activity of the proximal 5′f region of mERβ gene is able to define only the expression in the testis. Quantitative measurements of lacZ revealed virtually no expression in other ERβ-positive organs, such as lung, ovary or prostate, though a very low level of lacZ mRNA was detected in the epididymis. Other enhancer elements may control other aspects of tissue-specific expression. Intronic enhancers would be one possibility, since they have been reported to be essential for some types of tissue-specific gene expression [30,31].

Complex promoter organization involving multiple promoters seems to be a common feature among the nuclear hormone receptor gene family [8]. It is noteworthy that, despite a number of reports suggesting promoter activity in the upstream region of the nuclear hormone receptors based on *in vitro* assay, *in vivo* function of these promoters has not been proven yet, except for a proximal promoter of mouse ERα. The present study of ERβ promoter, which indicates that the 5′f region alone possesses very limited promoter activity for tissue-specific expression, provides further insight into promoter function in the nuclear receptor family.

Acknowledgments

This work was supported in part by a Grant-in-Aid (H16-Seikatsu) from the Ministry of Health, Labor and Welfare, Japan and a Grant-in-Aid (#17510046) from the Ministry of Education, Culture, Sports, Science and Technology, Japan.

References

[1] J.A. Gustafsson, Estrogen receptor beta—a new dimension in estrogen mechanism of action, J. Endocrinol. 163 (1999) 379–383.
[2] L. O'Donnell, K.M. Robertson, M.E. Jones, E.R. Simpson, Estrogen and spermatogenesis, Endocr. Rev. 22 (2001) 289–318.
[3] B.T. Akingbemi, Estrogen regulation of testicular function, Reprod. Biol. Endocrinol. 3 (2005) 51.
[4] K. Grandien, Determination of transcription start sites in the human estrogen receptor gene and identification of a novel, tissue-specific, estrogen receptor-mRNA isoform, Mol. Cell. Endocrinol. 116 (1996) 207–212.
[5] M. Kos, G. Reid, S. Denger, F. Gannon, Minireview: genomic organization of the human ERalpha gene promoter region, Mol. Endocrinol. 15 (2001) 2057–2063.
[6] G.B. Tremblay, A. Tremblay, N.G. Copeland, D.J. Gilbert, N.A. Jenkins, F. Labrie, V. Giguere, Cloning, chromosomal localization, and functional analysis of the murine estrogen receptor beta, Mol. Endocrinol. 11 (1997) 353–365.
[7] B. Freyschuss, K. Grandien, The 5′ flank of the rat estrogen receptor gene: structural characterization and evidence for tissue- and species-specific promoter utilization, J. Mol. Endocrinol. 17 (1996) 197–206.
[8] K. Grandien, A. Berkenstam, J.A. Gustafsson, The estrogen receptor gene: promoter organization and expression, Int. J. Biochem. Cell Biol. 29 (1997) 1343–1369.
[9] S. Hirata, T. Koh, M.N. Yamada, J. Kato, The novel untranslated first exon "exon 0N" of the rat estrogen receptor gene, Biochem. Biophys. Res. Commun. 225 (1996) 849–854.
[10] C. Tiffoche, C. Vaillant, D. Schausi, M.L. Thieulant, Novel intronic promoter in the rat ER alpha gene responsible for the transient transcription of a variant receptor, Endocrinology 142 (2001) 4106–4119.
[11] S. Hirata, T. Shoda, J. Kato, K. Hoshi, The multiple untranslated first exons system of the human estrogen receptor beta (ER beta) gene, J. Steroid Biochem. Mol. Biol. 78 (2001) 33–40.
[12] L.C. Li, C.C. Yeh, D. Nojima, R. Dahiya, Cloning and characterization of human estrogen receptor beta promoter, Biochem. Biophys. Res. Commun. 275 (2000) 682–689.
[13] N. Fujimoto, K. Asano, T. Usui, H. Honda, S. Kitamura, Cloning and characterization of the 5′-flanking region of the rat estrogen receptor beta gene, J. Steroid Biochem. Mol. Biol. 94 (2005) 15–21.
[14] O. Ishibashi, H. Kawashima, Cloning and characterization of the functional promoter of mouse estrogen receptor beta gene, Biochim. Biophys. Acta 1519 (2001) 223–229.
[15] E.H. Mercer, G.W. Hoyle, R.P. Kapur, R.L. Brinster, R.D. Palmiter, The dopamine beta-hydroxylase gene promoter directs expression of *E. coli* lacZ to sympathetic and other neurons in adult transgenic mice, Neuron 7 (1991) 703–716.
[16] T. Arimoto, Y. Takeishi, H. Takahashi, T. Shishido, T. Niizeki, Y. Koyama, R. Shiga, N. Nozaki, O. Nakajima, K. Nishimaru, J. Abe, M. Endoh, R.A. Walsh, K. Goto, I. Kubota, Cardiac-specific overexpression of diacylglycerol kinase zeta prevents Gq protein-coupled receptor agonist-induced cardiac hypertrophy in transgenic mice, Circulation 113 (2006) 60–66.
[17] J. Wakabayashi, K. Yomogida, O. Nakajima, K. Yoh, S. Takahashi, J.D. Engel, K. Ohneda, M. Yamamoto, GATA-1 testis activation region is essential for Sertoli cell-specific expression of GATA-1 gene in transgenic mouse, Genes Cells 8 (2003) 619–630.
[18] N. Fujimoto, K. Igarashi, J. Kanno, H. Honda, T. Inoue, Identification of estrogen-responsive genes in the GH3 cell line by cDNA microarray analysis, J. Steroid Biochem. Mol. Biol. 91 (2004) 121–129.
[19] R. Kindich, A.R. Florl, V. Jung, R. Engers, M. Muller, W.A. Schulz, B. Wullich, Application of a modified real-time PCR technique for relative gene copy number quantification to the determination of the relationship between NKX3.1 loss and MYC gain in prostate cancer, Clin. Chem. 51 (2005) 649–652.
[20] J.F. Couse, J. Lindzey, K. Grandien, J.A. Gustafsson, K.S. Korach, Tissue distribution and quantitative analysis of estrogen receptor-alpha (ERalpha) and estrogen receptor-beta (ERbeta) messenger ribonucleic acid in the wild-type and ERalpha-knockout mouse, Endocrinology 138 (1997) 4613–4621.
[21] K. Pettersson, J.A. Gustafsson, Role of estrogen receptor beta in estrogen action, Annu. Rev. Physiol. 63 (2001) 165–192.
[22] S. Mosselman, J. Polman, R. Dijkema, ER beta: identification and characterization of a novel human estrogen receptor, FEBS Lett. 392 (1996) 49–53.
[23] G.G. Kuiper, E. Enmark, H.M. Pelto, S. Nilsson, J.A. Gustafsson, Cloning of a novel receptor expressed in rat prostate and ovary, Proc. Natl. Acad. Sci. U.S.A. 93 (1996) 5925–5930.
[24] Q. Zhou, R. Nie, G.S. Prins, P.T. Saunders, B.S. Katzenellenbogen, R.A. Hess, Localization of androgen and estrogen receptors in adult male mouse reproductive tract, J. Androl. 23 (2002) 870–881.
[25] C.N. Mowa, T. Iwanaga, Expression of estrogen receptor-alpha and -beta mRNAs in the male reproductive system of the rat as revealed by in situ hybridization, J. Mol. Endocrinol. 26 (2001) 165–174.
[26] G. Pelletier, C. Labrie, F. Labrie, Localization of oestrogen receptor alpha, oestrogen receptor beta and androgen receptors in the rat reproductive organs, J. Endocrinol. 165 (2000) 359–370.
[27] S.F. Sneddon, N. Walther, P.T. Saunders, Expression of androgen and estrogen receptors in sertoli cells: studies using the mouse SK11 cell line, Endocrinology 146 (2005) 5304–5312.
[28] V. Rago, M. Maggiolini, A. Vivacqua, A. Palma, A. Carpino, Differential expression of estrogen receptors (ERalpha/ERbeta) in testis of mature and immature pigs, Anat. Rec. A: Discov. Mol. Cell Evol. Biol. 281 (2004) 1234–1239.
[29] L. Cicatiello, G. Cobellis, R. Addeo, M. Papa, L. Altucci, V. Sica, F. Bresciani, M. LeMeur, V.L. Kumar, P. Chambon, In vivo functional analysis of the mouse estrogen receptor gene promoter: a transgenic mouse model to study tissue-specific and developmental regulation of estrogen receptor gene transcription, Mol. Endocrinol. 9 (1995) 1077–1090.
[30] A. Kappel, V. Ronicke, A. Damert, I. Flamme, W. Risau, G. Breier, Identification of vascular endothelial growth factor (VEGF) receptor-2 (Flk-1) promoter/enhancer sequences sufficient for angioblast and endothelial cell-specific transcription in transgenic mice, Blood 93 (1999) 4284–4292.
[31] Y. Shima, M. Zubair, S. Ishihara, Y. Shinohara, S. Oka, S. Kimura, S. Okamoto, Y. Minokoshi, S. Suita, K. Morohashi, Ventromedial hypothalamic nucleus-specific enhancer of Ad4BP/SF-1 gene, Mol. Endocrinol. 19 (2005) 2812–2823.

FULL PAPER *Pathology*

Gene Expression Profiling and Cellular Distribution of Molecules with Altered Expression in the Hippocampal CA1 Region after Developmental Exposure to Anti-Thyroid Agents in Rats

Yukie SAEGUSA[1,2], Gye-Hyeong WOO[3], Hitoshi FUJIMOTO[3], Kaoru INOUE[3], Miwa TAKAHASHI[3], Masao HIROSE[3,4], Katsuhide IGARASHI[5], Jun KANNO[5], Kunitoshi MITSUMORI[1], Akiyoshi NISHIKAWA[3] and Makoto SHIBUTANI[1]*

[1]*Laboratory of Veterinary Pathology, Tokyo University of Agriculture and Technology, 3–5–8 Saiwai-cho, Fuchu-shi, Tokyo 183–8509,* [2]*Pathogenetic Veterinary Science, United Graduate School of Veterinary Sciences, Gifu University, 1–1 Yanagido, Gifu-shi, Gifu 501–1193,* [3]*Division of Pathology and* [5]*Division of Molecular Toxicology, National Institute of Health Sciences, 1–18–1 Kamiyoga, Setagaya-ku, Tokyo 158–8501 and* [4]*Food Safety Commission, Akasaka Park Bld. 22nd F., 5–2–20 Akasaka, Minato-ku, Tokyo 100–8989, Japan*

(Received 6 September 2009/Accepted 8 Octoberr 2009/Published online in J-STAGE 27 November 2009)

ABSTRACT. To determine whether developmental hypothyroidism causes permanent disruption of neuronal development, we first performed a global gene expression profiling study targeting hippocampal CA1 neurons in male rats at the end of maternal exposure to anti-thyroid agents on weaning (postnatal day 20). As a result, genes associated with nervous system development, zinc ion binding, apoptosis and cell adhesion were commonly up- or down-regulated. Genes related to calcium ion binding were up-regulated and those for myelination were often down-regulated. We, then, examined immunohistochemical cellular distribution of Ephrin type A receptor 5 (EphA5) and Tachykinin receptor (Tacr)-3, those selected based on the gene expression profiles, in the hippocampal formation at the adult stage (11-week-old) as well as at the end of exposure. At weaning, both EphA5- and Tacr3-immunoreactive cells with strong intensities appeared in the pyramidal cell layer or stratum oriens of the hippocampal CA1 region. Although the magnitude of the change was decreased at the adult stage, Tacr3 in the CA1 region showed a sustained increase in expressing cells until the adult stage after developmental hypothyroidism. On the other hand, EphA5-expressing cells did not show sustained increase at the adult stage. The results suggest that developmental hypothyroidism caused sustained neuronal expression of Tacr3 in the hippocampal CA1 region, probably reflecting a neuroprotective mechanism for mismigration.

KEY WORDS: developmental hypothyroidism, EphA5, hippocampal CA1 region, Tacr3.

J. Vet. Med. Sci. 72(2): 187–195, 2010

Thyroid hormones are essential for normal fetal and neonatal brain development. They control neuronal and glial proliferation in definitive brain regions and regulate neural migration and differentiation [12, 18, 21]. In humans, maternal hypothyroxinemia, early in pregnancy, may have adverse effects on fetal brain development and importantly, even mild-moderate hypothyroxinemia may result in suboptimal neurodevelopment [4]. These results may increase the concern of thyroid hormone-disrupting chemicals in the environment.

Experimentally, developmental hypothyroidism leads to growth retardation, neurological defects and impaired performance on a variety of behavioral learning actions [1, 2]. Rat offspring exposed maternally to anti-thyroid agents such as 6-propyl-2-thiouracil (PTU) show brain retardation, with impaired neuronal migration and white matter hypoplasia involving limited axonal myelination and oligodendrocytic accumulation [6, 8, 21]. The outcome of this type of brain retardation is permanent and is accompanied by apparent structural and functional abnormalities. However, it is still unclear whether the molecular aberrations remain in the retarded brain after maturation.

Histological lesion-specific gene expression profiling provides valuable information on the mechanisms underlying lesion development. We have established molecular analysis methods for DNA, RNA and proteins in paraffin-embedded small tissue specimens utilizing an organic solvent-based fixative, methacarn, with high performance close to that achieved with unfixed frozen tissue specimens [22, 26, 27]. We have previously applied these techniques to analyze global gene expression changes in microdissected lesions [23, 28].

Hippocampal CA1 region is a well-known target of developmental hypothyroidism [8], and we, in our recent study, detected a distribution variability of hippocampal CA1 pyramidal neurons reflecting mismigration in rat offspring at the adult stage after developmental exposure to anti-thyroid agents [24]. The present study was performed to determine whether developmental hypothyroidism triggers sustained aberrations in neuronal development associated with neuronal mismigration until the adult stage. For this purpose, we first performed a global gene expression profiling of the CA1-pyramidal cell layer in rat offspring at the end of developmental exposure to anti-thyroid agents. To distinguish chemical-specific expression changes from hypothyroidism-linked ones, two different anti-thyroid

* CORRESPONDENCE TO: SHIBUTANI, M., Laboratory of Veterinary Pathology, Tokyo University of Agriculture and Technology, 3–5–8 Saiwai-cho, Fuchu-shi, Tokyo 183–8509, Japan.
e-mail: mshibuta@cc.tuat.ac.jp

agents, PTU and 2-mercapto-1-methylimidazole (MMI), were used, and dose-related responses were also examined with PTU. To extract the neuronal cell layer-specific gene expression profile, microdissection technique was applied for microarray analysis. Based on the expression profiles obtained, cellular localization of the molecules showing altered expression were then immunohistochemically examined in the hippocampus at the adult stage as well as at the end of the developmental exposure.

MATERIALS AND METHODS

Chemicals and animals: 6-propyl-2-thiouracil (PTU; CAS No. 51–52–5) and methimazole (2-mercapto-1-methylimidazole: MMI; CAS No. 60–56–0) were obtained from Sigma Chemical Co. (St. Louis, MO, U.S.A.). Pregnant Crj:CD®(SD)IGS rats were purchased from Charles River Japan Inc. (Yokohama, Japan) at gestation day (GD) 3 (appearance of vaginal plugs was designated as GD 0). Animals were housed individually in polycarbonate cages with wood chip bedding, maintained in an air-conditioned animal room (temperature: 24 ± 1°C; relative humidity: 55 ± 5%) with a 12-hr light/dark cycle and allowed *ad libitum* access to food and tap water. A soy-free diet (Oriental Yeast Co., Ltd., Tokyo, Japan) was chosen as the basal diet for the maternal animals to eliminate possible phytoestrogen effects [10], and water was given *ad libitum* throughout the experimental period including the 1-week acclimation period.

Animal experiments: The animal experiments were identical to those in a previous study [24]. In brief, maternal animals were randomly divided into four groups including untreated controls. Eight dams per group were treated with 3 or 12 ppm of PTU or 200 ppm of MMI in the drinking water from GD 10 to postnatal day (PND) 20 (PND 0: the day of delivery). On PND 2, the litters were culled randomly, leaving four male and four female offspring. On PND 20, 20 male and 20 female offspring (at least one male and one female per dam) per group were subjected to prepubertal necropsy [13, 24].

The remaining animals were maintained until postnatal week (PNW) 11. All offspring consumed the CRF-1 basal diet and tap water *ad libitum* from PND 21 onwards. At PNW 11, all pups were subjected to adult stage necropsy [13, 24].

All animals used in the present study were weighed and sacrificed by exsanguination from the abdominal aorta under deep anesthesia. These protocols were reviewed in terms of animal welfare and approved by the Animal Care and Use Committee of the National Institute of Health Sciences, Japan.

Preparation of tissue specimens and microdissection: For microarray and subsequent real-time RT-PCR analyses, the whole brain of male offspring was removed at prepubertal necropsy on PND 20 (n=4/group) and was fixed with methacarn solution for 2 hr at 4°C [22]. Coronal brain slices taken at the position of –3.5 mm from the bregma were dehydrated and embedded in paraffin. The embedded tissue blocks were stored at 4°C until tissue sectioning for microdissection [9].

For microdissection, 4-μm-thick sections between ten 20 μm-thick serial sections were prepared. The 4 μm-thick sections were stained with hematoxylin and eosin for confirmation of anatomical orientation of the hippocampal substructure to aid microdissection. The 20 μm-thick sections were mounted onto PEN-foil film (Leica Microsystems GmbH, Welzlar, Germany) overlaid on glass slides, dried in an incubator overnight at 37°C, and then stained using an LCM staining kit (Ambion, Inc., Austin, TX, U.S.A.). Bilateral sides of the hippocampal CA1 pyramidal cell layer in the sections were subjected to laser microbeam microdissection (Leica Microsystems GmbH) (Fig. 1). Twenty sections from each animal were used for microdissection, and the bilateral microdissected samples were collected and stored in separate 1.5-m*l* sample tubes at –80°C until the extraction of total RNA.

RNA preparation, amplification and microarray analysis: Total RNA extraction from hippocampal CA1 samples, quantitation of the RNA yield, and amplification of RNA samples were performed using previously described methods [9, 28].

For microarray analysis, second-round-amplified biotin-labeled antisense RNAs were subjected to hybridization with a GeneChip® Rat Genome 230 2.0 Array (Affymetrix, Inc., Santa Clara, CA, U.S.A.), as previously described [28].

The selection of genes and normalization of the expression data were performed using GeneSpring® software (ver7.2, Silicon Genetics, Redwood City, CA, U.S.A.). Per chip normalization was performed according to a previously described method [28]. Genes showing signals judged to be "absent" in all eight samples of untreated controls and in the anti-thyroid agent-exposed group were excluded. Genes

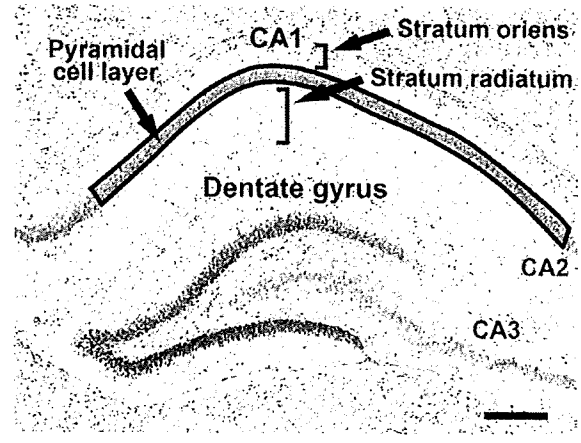

Fig. 1. Overview of the hippocampal formation of a male rat at postnatal day 20 stained with hematoxylin and eosin. Bar=200 μm. The CA1 pyramidal cell layer, enclosed by a solid line, was microdissected for the microarray and subsequent real-time RT-PCR analyses. The number of cells immunoreactive for the candidate molecules in this area was normalized for the length of CA1 used.

showing expression changes with differences of at least twofold in magnitude from the untreated controls were selected, and the "presence" signal in more than 3/4 of samples in each group showing higher expression values were selected. Genes showing altered expression in common in the anti-thyroid agent-exposed groups were also selected.

Real-time RT-PCR: Quantitative real-time RT-PCR was performed to confirm the expression values obtained with microarrays using an ABI Prism 7000 Sequence Detection System (Applied Biosystems Japan, Tokyo, Japan). Genes those showing altered expression (≥2-fold, ≤0.5-fold) in common in the anti-thyroid agent-exposed groups as compared with untreated control offspring were randomly selected, irrespective of the presence or absence of statistically significant difference. As a result, the following seven genes (four up-regulated and three down-regulated) with known function were selected as targets: Tachykinin receptor 3 (*Tacr3*), Calbindin 1, Slit homolog 2 (Drosophila) and Pleomorphic adenoma gene-like 1 (*Plagl1*) as up-regulated examples, and Myelin-associated oligodendrocytic basic protein (*Mobp*), Endothelial differentiation, sphingolipid G-protein-coupled receptor, 8 and CCAAT/enhancer binding protein as down-regulated. RT was performed using first-round antisense RNAs prepared for microarray analysis. For real-time PCR analysis of the genes selected, ABI Assays-on-Demand™ TaqMan® probe and primer sets from Applied Biosystems (available at https://products.appliedbiosystems.com/ab/en/US/adirect/ab?cmd=catNavigate2&catID=601267)(n=4/group) were used. For quantification of the expression data, a standard curve method was applied. The expression values were normalized to two housekeeping genes, Glyceraldehyde 3-phosphate dehydrogenase and Hypoxanthine-guanine phosphoribosyltransferase.

Immunohistochemistry: To evaluate the immunohistochemical distribution of the molecules selected by microarray analysis, the brains of male pups obtained at PND 20 or PNW 11 were fixed in Bouin's solution at room temperature overnight. Six animals were used as untreated controls, six for 200 ppm MMI, eight for 3 ppm PTU, and nine for 12 ppm PTU on PND 20. On PNW 11, 10 animals were used as untreated controls and 10 for 200 ppm MMI, nine for 3 ppm PTU, and six for 12 ppm PTU.

Immunohistochemistry was performed on the brain tissue sections of PND 20 and PNW 11 animals with antibodies against Ephrin type A receptor 5 (EphA5; rabbit IgG, 1:50; Abcam, Cambridge, U.K.) and Tacr3 (rabbit polyclonal antibody, 1:3,000, Novus Biologicals, Inc., Littleton, CO, U.S.A.), which were incubated with the tissue sections overnight at 4°C. Antigen retrieval treatment was not performed for these antigens. Immunodetection was carried out using a VECTASTAIN® Elite ABC kit (Vector Laboratories Inc., Burlingame, CA, U.S.A.) with 3,3'-diaminobenzidine/H_2O_2 as the chromogen, as previously described [23]. The sections were then counterstained with hematoxylin and coverslipped for microscopic examination.

With regard to EphA5, *Efna5*, a gene encoding the representative ligand for this receptor molecule [5], was found to be up-regulated (≥2-fold) by microarray analysis in all of the groups exposed to anti-thyroid agents in the present study (Table 1). Because distribution of EphA5 has been confirmed in the pyramidal cells of the hippocampal CA1 region at both developmental and adult stages in mice and at adult stage in humans [3, 17], we selected this molecule to examine distribution changes in the present study. Tacr3 was also up-regulated in all of the MMI and PTU groups by microarray analysis and real-time RT-PCR in the present study (Table 1). Expression of Tacr3 in the hippocampal CA1 pyramidal neurons has also been confirmed in rats [11], and therefore, we also selected this molecule for examination in the expression changes in the present study.

Morphometry of immunolocalized cells and apoptotic cells: EphA5- or Tacr3-immunoreactive cells distributed in the pyramidal cell layer or stratum oriens of the hippocampal CA1 region were bilaterally counted and normalized to the number in the length of the CA1 region measured (Fig. 1). Tacr3-immunoreactive cells in the subgranular zone of the dentate gyrus were also bilaterally counted and normalized for the number in the length of the granular zone measured. For quantitative measurement of each immunoreactive cellular component, digital photomicrographs at 100-fold magnification were taken using a BX51 microscope (Olympus Optical Co., Ltd., Tokyo, Japan) attached to a DP70 Digital Camera System (Olympus Optical Co., Ltd.), and quantitative measurements were performed using the WinROOF image analysis software package (version 5.7, Mitani Corp., Fukui, Japan).

Statistical analysis: Numerical data of the number of immunoreactive cells were assessed using Student's *t*-test to compare the untreated controls with each of the anti-thyroid agent-exposed groups when the variance was homogenous among the groups using a test for equal variance. If a significant difference in variance was observed, Aspin-Welch's *t*-test was used instead. The data for gene expression levels from real-time RT-PCR analysis were analyzed by the Kruskal-Wallis test, followed by Bartlett's test. When statistically significant differences were indicated, Dunnett's multiple test was used for comparisons with the untreated controls. For the microarray data, statistical analysis was performed with GeneSpring® software, and the significance of gene expression changes was analyzed by Student's *t*-test or ANOVA between the untreated controls and each of the anti-thyroid agent-exposed groups.

RESULTS

Microarray analysis: Figure 2 shows the Venn diagram of genes showing altered expression in the microdissected CA1 pyramidal neurons in the exposure groups in combination or individually in each exposure group. Many genes were found to be up- or down-regulated in common in two of the three groups. The numbers of genes classified into common categories between the groups or individually in each group were similar in terms of up- and down-regulated genes. The number of genes showing up- or down-regula-

Table 1. List of representative genes showing up- or down-regulation common to 2-mercapto-1-methylimidazole (MMI), 3 and 12 ppm 6-propyl-2-thiouracil (PTU) (≥2-fold, ≤0.5-fold)

Gene function	Accession No.	Gene title	Symbol	MMI	3 ppm PTU	12 ppm PTU
Up-regulated genes (of 119 genes in total)						
Nervous system development	AI101660	Slit homolog 2 (Drosophila)	Slit2	3.04	2.62	7.08
Nervous system development	NM_024358.1	Notch gene homolog 2 (Drosophila)	Notch2	2.52	2.01	2.02
Nervous system development	AW527295	Ephrin A5	Efna5	3.12	3.46	4.31
Nervous system development	NM_053465.1	Fucosyltransferase 9	Fut9	2.13	6.75	2.11
Nervous system development	BE106256	Sparc/osteonectin, cwcv and kazal-like domains proteoglycan 1	Spock1	3.22	3.13	2.15
Calcium ion binding	X04280.1	Calbindin 1	Calb1	4.48	4.85	9.00
Calcium ion binding	BM386119	UDP-N-acetyl-alpha-D-galactosamine:polypeptide N-acetylgalactosaminyltransferase 3 (GalNAc-T3)	Galnt3	2.43	2.30	2.63
Calcium ion binding	BI279663	Desmocollin 2	Dsc2	2.82	2.04	5.62
Calcium ion binding	AI105369	Calmodulin-like 4	Calml4	3.40	2.25	5.59
Zinc ion binding	BE098686	Similar to Tnf receptor-associated factor 1	LOC687813	3.10	2.04	2.78
Zinc ion binding	BF562032	RAN binding protein 2	Ranbp2	3.49	2.67	2.78
Zinc ion binding	BF397925	ADAMTS-like 1	Adamtsl1	6.22	2.55	7.63
Zinc ion binding	BF395606	Splicing factor, arginine/serine-rich 7	Sfrs7	4.93	2.06	2.90
Apoptosis	NM_012760.1	Pleomorphic adenoma gene-like 1	Plagl1	3.10	4.28	6.86
Apoptosis	NM_057130.1	Harakiri, BCL2 interacting protein (contains only BH3 domain)	Hrk	2.63	2.73	3.18
Cell Adhesion	AA850909	Poliovirus receptor-related 2	Pvrl2	4.74	2.46	2.61
Cell Adhesion	AA819731	Hyaluronan and proteoglycan link protein 4	Hapln4	4.13	6.67	3.46
Cell Adhesion	BI287851	Collagen, type VI, alpha 2	Col6a2	3.45	2.19	5.12
Ion channel activity	AA851939	FXYD domain-containing ion transport regulator 6	Fxyd6	4.73	2.61	7.85
Other	NM_017053.1	Tachykinin receptor 3	Tacr3	7.32	6.19	12.49
Down-regulated genes (of 97 genes in total)						
Nervous system development	NM_031018.1	Activating transcription factor 2	Atf2	0.41	0.36	0.36
Neuron migration	BF390065	Roundabout homolog 3 (Drosophila)	Robo3	0.06	0.31	0.04
Neuron differentiation	AF115249.1	Endothelial differentiation, sphingolipid G-protein-coupled receptor, 8	Edg8	0.40	0.06	0.08
Neuron differentiation	NM_024125.1	CCAAT/enhancer binding protein (C/EBP), beta	Cebpb	0.31	0.43	0.26
Myelination	X89638.1	Myelin-associated oligodendrocytic basic protein	Mobp	0.35	0.18	0.12
Myelination	NM_017190.1	Myelin-associated glycoprotein	Mag	0.47	0.36	0.29
Myelination	NM_022668.1	Myelin oligodendrocyte glycoprotein	Mog	0.44	0.32	0.19
Myelination	NM_012798.1	Mal, T-cell differentiation protein	Mal	0.37	0.28	0.28
Myelination	AA945178	Signal recognition particle receptor, B subunit transferrin	Srprb Tf	0.33	0.27	0.15
Zinc ion binding	NM_012566.1	Growth factor independent 1 transcription repressor	Gfi1	0.20	0.44	0.41
Zinc ion binding	AW529624	Zinc finger protein 91	Zfp91	0.33	0.32	0.38
Actin binding	AW522439	Ermin, ERM-like protein	Ermn	0.43	0.42	0.28
Apoptosis	BG377720	Solute carrier family 5 (sodium/glucose cotransporter), member 11	Slc5a11	0.25	0.19	0.19
Apoptosis	U21955.1	Eph receptor A	Epha7	0.34	0.48	0.18
Cell Adhesion	BM391100	Mucin 4, cell surface associated	Muc4	0.43	0.36	0.27
Other	AW435010	Protein tyrosine phosphatase, non-receptor type 3	Ptpn3	0.38	0.46	0.36
Other	AF312319.1	gamma-aminobutyric acid (GABA) B receptor 1	Gabbr1	0.33	0.41	0.39
Other	NM_053936.1	Endothelial differentiation, lysophosphatidic acid G-protein-coupled receptor, 2	Edg2	0.47	0.31	0.31

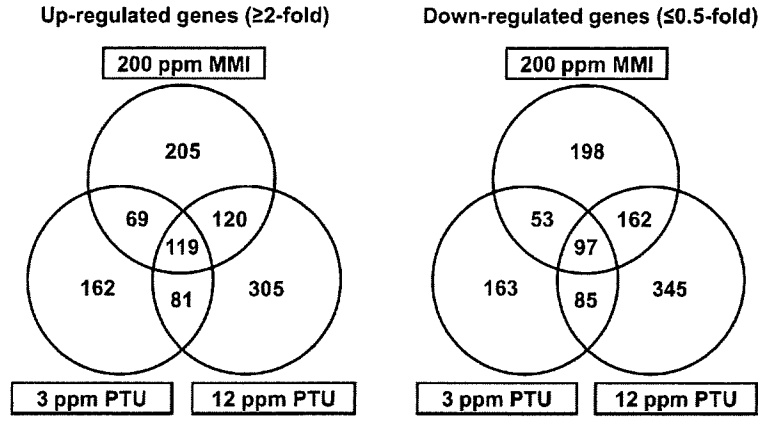

Fig. 2. Venn diagram of gene populations showing altered expression in the hippocampal CA1 pyramidal cell layer at postnatal day 20 in response to maternal exposure to propylthiouracil and/or 2-mercapto-1-methylimidazole compared with the untreated controls. (Left) Up-regulated genes (≥2-fold). (Right) Down-regulated genes (≤0.5-fold). Abbreviations: MMI, 2-mercapto-1-methylimidazole; PTU, 6-propyl-2-thiouracil.

Table 2. Validation of microarray data by real-time RT-PCR

Gene	200 ppm MMI			3 ppm PTU			12 ppm PTU		
	Microarray	Real-time RT-PCR normalized to		Microarray	Real-time RT-PCR normalized to		Microarray	Real-time RT-PCR normalized to	
		Hprt[a)]	Gapdh[b)]		Hprt	Gapdh		Hprt	Gapdh
Tacr3[c)]	7.32 ± 2.21**	4.29 ± 1.27	4.08 ± 1.15*	6.19 ± 2.19**	3.46 ± 1.42	3.76 ± 1.51*	12.49 ± 1.56**	9.23 ± 3.00**	8.81 ± 1.60**
Calb1[d)]	4.48 ± 0.66*	3.96 ± 0.74	3.67 ± 0.16	4.85 ± 2.53*	4.74 ± 2.48	4.93 ± 3.79	9.00 ± 1.85**	11.13 ± 2.13**	10.53 ± 3.26**
Slit2[e)]	3.04 ± 0.79	2.83 ± 0.90	4.08 ± 1.15*	2.62 ± 1.16	1.33 ± 0.67	3.67 ± 1.51*	7.08 ± 2.15**	4.72 ± 2.57**	8.81 ± 1.60**
Plgl1[f)]	3.10 ± 1.57	12.67 ± 5.00	11.5 ± 7.50	4.28 ± 2.88	18.33 ± 6.00	19.00 ± 9.00*	6.86 ± 2.85**	30.67 ± 5.33**	27.00 ± 8.00**
Mobp[g)]	0.35 ± 0.15**	0.6 ± 0.22*	0.52 ± 0.16**	0.18 ± 0.07**	0.24 ± 0.07**	0.24 ± 0.05**	0.12 ± 0.02**	0.18 ± 0.04**	0.16 ± 0.04**
Edg8[h)]	0.40 ± 0.11*	0.49 ± 0.16*	0.43 ± 0.13*	0.06 ± 0.05**	0.29 ± 0.10**	0.28 ± 0.08**	0.08 ± 0.07**	0.21 ± 0.07**	0.18 ± 0.03**
Cebpb[i)]	0.31 ± 0.06**	0.43 ± 0.04**	0.38 ± 0.06**	0.43 ± 0.18**	0.77 ± 0.07	0.76 ± 0.10	0.26 ± 0.04**	0.39 ± 0.16**	0.35 ± 0.22**

a) Hprt, Hypoxanthine-guanine phosphoribosyltransferase; b) Gapdh, Glyceraldehyde 3-phosphate dehydrogenase; c) Tacr3, Tachykinin receptor 3; d) Calb1, Calbindin 1; e) Slit2, Slit homolog 2 (Drosophila); f) Plgl1, Pleomorphic adenoma gene-like 1; g) Mobp, Myelin-associated oligodendrocytic basic protein; h) Edg8, Endothelial differentiation, sphingolipid G-protein-coupled receptor, 8; i) Cebpb, CCAAT/enhancer binding protein (C/EBP), beta.

Values are mean ± SD (n=4) relative to the expression level in the untreated controls. Real-time RT-PCR analysis of Hprt and Gapdh was performed in the analysis of each target gene.

*, **: Significantly different from the untreated controls at $P<0.05$ and $P<0.01$, respectively (Dunnett's multiple comparison test).

tion in response to 12 ppm PTU was approximately 2-fold higher than that with 3 ppm PTU. The number of genes showing up- or down-regulation in response to 200 ppm MMI was in between that elicited by 3 or 12 ppm PTU. One-hundred nineteen genes were up-regulated in common by MMI and PTU, with PTU showing up-regulation from 3 ppm. On the other hand, 97 genes showed down-regulation in all MMI and PTU groups. Representative genes showing up- or down-regulation in all three groups are shown in the Table 1. Among the genes listed, genes associated with nervous system development, zinc ion binding, apoptosis and cell adhesion were commonly up- or down-regulated. Genes related to calcium ion binding were found to be up-regulated and those for myelination were often down-regulated.

Real-time RT-PCR analysis: For confirmation of the microarray data, four genes that were up-regulated and three that were down-regulated in response to anti-thyroid agents were selected for mRNA expression analysis by real-time RT-PCR and the results are summarized in Table 2.

In all exposure groups, many of the expression changes were similar in the two analysis systems, except for much higher expression of *Plagl1* in all exposure groups by real-time RT-PCR as compared with findings from the microarray system.

Although we performed expression analysis of *Efna5* by real-time RT-PCR, expression values were rather low with great variability between samples, and therefore, reliable quantitative data could not be obtained (data not shown).

Immunolocalization of EphA5 and Tacr3 in the hippoc-

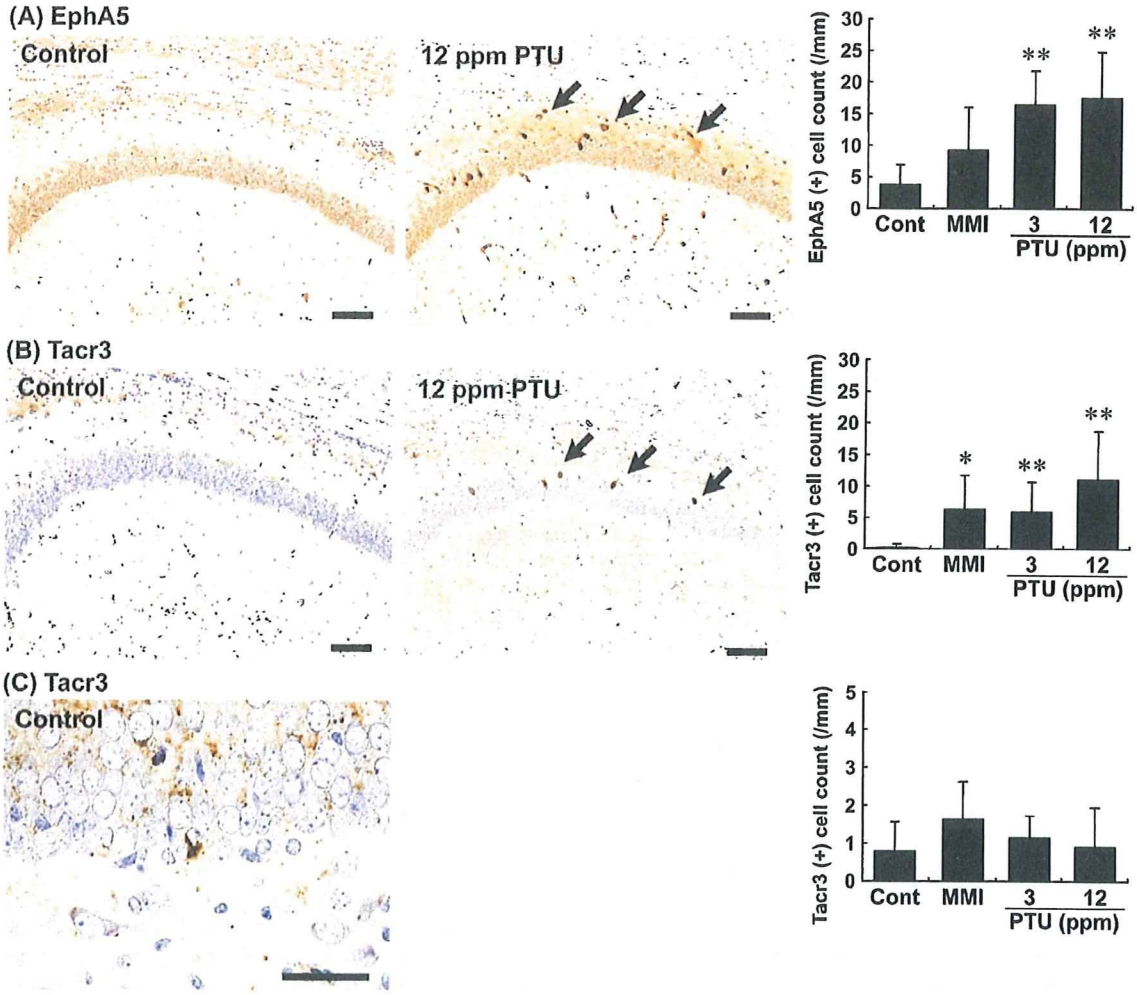

Fig. 3. Distribution of immunoreactive cells for EphA5 and Tacr3 in the hippocampal formation in rats at PND 20 after maternal exposure to anti-thyroid agents. (A) EphA5-immunoreactive cells with strong intensity located within the pyramidal cell layer and stratum oriens of the hippocampal CA1 region (arrows). Note the higher number of EphA5-positive cells in a case exposed to 12 ppm PTU (Right) as compared with the control animal (Left). Bar =100 μm. The graph shows the number of EphA5-positive cells/unit length (mm) of the CA1 region of the bilateral hemispheres. ** $P<0.01$ versus untreated controls (Student's *t*-test). (B) Tacr3-immunoreactive cells with strong intensity located within the pyramidal cell layer and stratum oriens of the hippocampal CA1 region (arrows). Note the higher number of Tacr3-positive cells in a case exposed to 12 ppm PTU (Right) as compared with the control animal (Left). Bar =100 μm. The graph shows the number of Tacr3-positive cells/unit length (mm) of the CA1 region of bilateral hemispheres. * $P<0.05$, ** $P<0.01$ versus untreated controls (Student's *t*-test). (C) Tacr3-immunoreactive cells located in the subgranular zone of the dentate gyrus. Bar =50 μm. The graph shows the number of Tacr3-positive cells/unit length (mm) of the subgranular zone of bilateral hemispheres. Abbreviations: EphA5, Ephrin type A receptor 5; MMI, 2-mercapto-1-methylimidazole; PTU, 6-propyl-2-thiouracil, Tacr3, Tachykinin receptor 3.

ampal formation: Immunohistochemical localization of EphA5 and Tacr3 in the hippocampal formation was examined at PND 20 and PNW 11.

On PND 20, EphA5 showed weak immunoreactivity in the pyramidal neurons throughout the hippocampal formation in the untreated controls. This immunoreactivity was unchanged by exposure to anti-thyroid agents. On the other hand, very sparse distribution of strongly immunoreactive cells for EphA5 was observed in the region of the CA1 pyramidal cell layer and stratum oriens in the untreated control animals, but immunoreactive cells were significantly increased showing scattered distribution by PTU at both 3 and 12 ppm (Fig. 3A). MMI-exposed animals also showed a small increase in the number of strongly positive cells with EphA5. Increased intensity in immunoreactivity of EphA5 was also observed in the gray matter consisting of neuropil at the stratum oriens of the CA1 region (Fig. 3A), and also in the molecular layer of the dentate gyrus at PND 20 after exposure to anti-thyroid agents, especially in PTU-exposed groups (data not shown).

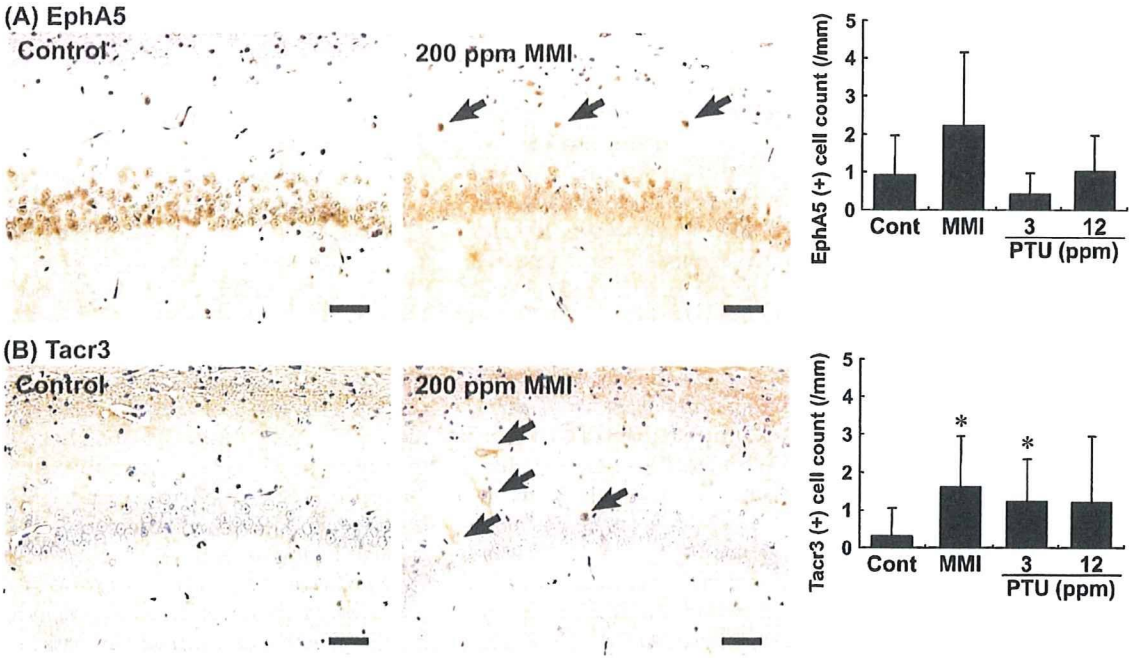

Fig. 4. Distribution of immunoreactive cells for EphA5 and Tacr3 in the hippocampal formation at PNW 11 of rats exposed maternally to anti-thyroid agents. (A) EphA5-immunoreactive cells with moderate staining intensity located within the pyramidal cell layer and stratum oriens of the hippocampal CA1 region. EphA5-positive cells in a case exposed to 200 ppm MMI (Right) as compared with the control animal (Left). The arrows show positive cells. Bar =50 μm. The graph shows the number of EphA5-positive cells/unit length (mm) of the CA1 region of the bilateral hemispheres. (B) Tacr3-immunoreactive cells with weak to moderate staining intensity located within the pyramidal cell layer and stratum oriens of the hippocampal CA1 region (arrows). Immunoreactivity is rather faint as compared with that observed at PND 20. Note the higher number of Tacr3-positive cells in a case exposed to 200 ppm MMI (Right) as compared with the control animal (Left). Bar =50 μm. The graph shows the number of Tacr3-positive cells/unit length (mm) of the CA1 region of bilateral hemispheres. * $P<0.05$ versus untreated controls (Student's *t*-test). Abbreviations: EphA5, Ephrin type A receptor 5; MMI, 2-mercapto-1-methylimidazole; PTU, 6-propyl-2-thiouracil; Tacr3, Tachykinin receptor 3.

With regards to Tacr3, the number of positive cells was increased with a scattered distribution showing strong intensity in the CA1 region similarly to that of EphA5 in the animals exposed to MMI or PTU on PND 20, but they were mostly absent in the untreated controls (Fig. 3B). Similarly, Tacr3-immunoreactive cells were sparse in the subgranular zone of the dentate gyrus in the MMI and PTU-exposed animals and in the untreated controls, but there were no differences in the number of positive cells as compared with the untreated controls (Fig. 3C). In addition, increased intensity in neuropil-immunoreactivity of Tacr3 was also observed in the strata oriens and radiatum of the CA1 region in all exposure groups of anti-thyroid agents (Fig. 3B).

On PNW 11, EphA5 showed weak immunoreactivity in the pyramidal neurons throughout the hippocampal formation in the untreated controls. This immunoreactivity was unchanged by exposure to anti-thyroid agents. EphA5-immunoreactive cells with moderate staining intensity were very sparsely observed in the region of the CA1 pyramidal cell layer and stratum oriens in the untreated control animals. There was no statistically significant increase in the number of these immunoreactive cells after exposure to PTU, while animals exposed to MMI showed a tendency for an increased number of immunoreactive cells (Fig. 4A). Increased neuropil-immunoreactivity of EphA5 as observed at PND 20 in exposure groups of anti-thyroid agents was mostly disappeared at PNW 11 (data not shown).

As well as at PND 20, Tacr3-immunoreactive cells were mostly absent in the untreated controls at PNW 11; however, a few immunoreactive cells with weak to moderate intensity were observed in the stratum oriens of the CA1 region in the animals exposed to anti-thyroid agents. There was a statistically significant difference in the animals treated with MMI or 3 ppm PTU compared with the untreated controls (Fig. 4B). Although the change was non-significant and lacked dose-dependence, 12 ppm PTU also showed an increasing tendency in the number of Tacr3-immunoreactive cells. In addition, increased neuropil-immunoreactivity of Tacr3 as observed at PND 20 in exposure groups of anti-thyroid agents was mostly disappeared at PNW 11 (data not shown).

DISCUSSION

In our recent study using rats [24], after maternal exposure to MMI or PTU, we detected typical hypothyroidism-related changes in the thyroid-related hormone levels, and hippocampal CA1 pyramidal neurons due to neuronal mismigration, as previously reported [8]. We also observed white matter changes, which seem to be due to impaired oligodendroglial development [6, 21]. To visualize molecules related to impaired neuronal development, microdissected CA1 region-specific global gene expression profiling was performed in the present study using the same animals that were used in our previous study. Two recently published studies have used microarrays to examine the expression profiles in the cerebral cortex and hippocampus of genes linked to developmental hypothyroidism caused by maternal PTU-exposure [7, 19]. In accordance with these studies, the genes that were significantly down-regulated in the present study included those that play roles in myelination, such as *Mobp* and myelin-associated glycoprotein, suggestive of the reflection of suppressed myelination by developmental hypothyroidism [21]. However, the genes that were found to be up-regulated on microdissected CA1 pyramidal cell layer, including *Efna5* and *Tacr3*, in the present study, have not been identified in previous studies. This difference may be related to the target tissues collected and the methods used, including microdissection of CA1 pyramidal cell layer from paraffin-embedded sections in the present study versus manual dissection of the cortical tissues from unfixed tissues in the previous studies.

EphA5 is a tyrosine kinase receptor that is almost exclusively expressed in the nervous system [15]. EphA5 and its ligand are important in mediating axon guidance, topographic projection, development, cell migration and the plasticity of limbic structures [15]. In addition, the transient expression of EphA5 during development is correlated with early neurogenesis and the migration of differentiated cells in the midbrain [3]. Thus, although expression of EphA5 was mostly weak in the euthyroid CA1 pyramidal neurons at PND 20, the increased number of EphA5-expressing cells with strong intensity in the CA1 region during developmental hypothyroidism in the present study reflects the neuronal mismigration caused by anti-thyroid agents. However, this increase was recovered after cessation of developmental hypothyroidism. Ephrins and their receptors are recently identified molecules and functional relationship between subfamily proteins is largely unknown; however, we, in the present study, found down-regulation of Epha7, another subfamily ephrin receptor, in all exposure groups of anti-thyroid agents (Table 1).

Tacr3, a member of the mammalian tachykinin peptide neurotransmitter/neuromodulator receptor family, is predominantly expressed in neurons in both the peripheral and central nervous systems, including the hippocampus [25]. There is increasing evidence of the role of Tacr3 on the survival and function of dopaminergic neurons. The survival of mesencephalic dopaminergic neurons during development largely depends on excitatory inputs, and tachykinins, through their receptors, are reported to play role in excitation [20]. On the other hand, senktide, a Tacr3 agonist, activates dopaminergic neurons to stimulate the release of dopamine and serotonin, and hyperlocomotion in gerbils [14]. Abnormal excitatory action of D_2-like receptor, one of the major subtypes of dopaminergic receptors, was observed on glutamatergic transmission in the CA1 synapses in the adult stage of rats after developmental hypothyroidism, suggesting a permanent disruption of synaptic integration in the CA1 neural networks [16]. While the role of Tacr3 in the hippocampal CA1 region during development is not clear, the increase in Tacr3-positive cells with strong intensity in this region during developmental hypothyroidism suggests a cell survival effect of tachykinin-3. Although the magnitude of the change was decreased, as compared with that at the end of the developmental hypothyroidism, the increased number of Tacr3-positive cells in the CA1 region of MMI and 3 ppm PTU-exposed animals may be an outcome of permanent disruption of synaptic integration, as described by Oh-Nishi *et al.* [16]. However, sparse distribution of Tacr3-positive cells may reflect that impairment sustained in a small population of aberrantly migrated neurons.

In conclusion, in this study, we have shown gene expression profiles showing altered expression in response to developmental hypothyroidism by analysis on microdissected hippocampal CA1 pyramidal cell layer in rats. Immunohistochemical analysis of the two candidate molecules revealed that developmental hypothyroidism until weaning is associated with the persistence of Tacr3-expressing neurons until the adult stage in the CA1 region, suggestive of the reflection of permanent disruption of synaptic integration. These findings probably reflect a mechanism to facilitate cell survival of aberrantly developed neurons due to mismigration.

ACKNOWLEDGMENT(S). We thank Miss Tomomi Morikawa for her technical assistance in conducting the animal study. We also thank Mrs. Shigeko Suzuki and Miss Ayako Kaneko for their technical assistance in preparing the histological specimens. This work was supported in part by Health and Labour Sciences Research Grants (Research on Risk of Chemical Substances) from the Ministry of Health, Labour and Welfare of Japan. All of the authors disclose that there are no conflicts of interest that could inappropriately influence the outcomes of the present study.

REFERENCES

1. Akaike, M., Kato, N., Ohno, H. and Kobayashi, T. 1991. Hyperactivity and spatial maze learning impairment of adult rats with temporary neonatal hypothyroidism. *Neurotoxicol. Teratol.* **13**: 317–322.
2. Comer, C. P. and Norton, S. 1982. Effects of perinatal methimazole exposure on a developmental test battery for neurobehavioral toxicity in rats. *Toxicol. Appl. Pharmacol.* **63**: 133–141.
3. Cooper, M. A., Crockett, D. P., Nowakowski, R. S., Gale, N. W. and Zhou, R. 2009. Distribution of EphA5 receptor protein

in the developing and adult mouse nervous system. *J. Comp. Neurol.* **514**: 310–328.
4. de Escobar, G. M., Obregón, M. J. and del Rey, F. E. 2007. Iodine deficiency and brain development in the first half of pregnancy. *Public Health Nutr.* **10**: 1554–1570.
5. Gerlai, R., Shinsky, N., Shih, A., Williams, P., Winer, J., Armanini, M., Cairns, B., Winslow, J., Gao, W. and Phillips, H. S. 1999. Regulation of learning by EphA receptors: a protein targeting study. *J. Neurosci.* **19**: 9538–9549.
6. Goodman, J. H. and Gilbert, M. E. 2007. Modest thyroid hormone insufficiency during development induces a cellular malformation in the corpus callosum: a model of cortical dysplasia. *Endocrinology* **148**: 2593–2597.
7. Kobayashi, K., Akune, H., Sumida, K., Saito, K., Yoshioka, T. and Tsuji, R. 2009. Perinatal exposure to PTU decreases expression of Arc, Homer 1, Egr 1 and Kcna 1 in the rat cerebral cortex and hippocampus. *Brain Res.* **1264**: 24–32.
8. Lavado-Autric, R., Ausó, E., García-Velasco, J. V., Arufe Mdel, C., Escobar del Rey, F., Berbel, P. and Morreale de Escobar, G. 2003. Early maternal hypothyroxinemia alters histogenesis and cerebral cortex cytoarchitecture of the progeny. *J. Clin. Invest.* **111**: 954–957.
9. Lee, K-Y., Shibutani, M., Inoue, K., Kuroiwa, K., U, M., Woo, G-H. and Hirose, M. 2006. Methacarn fixation—Effects of tissue processing and storage conditions on detection of mRNAs and proteins in paraffin-embedded tissues. *Anal. Biochem.* **351**: 36–43.
10. Masutomi, N., Shibutani, M., Takagi, H., Uneyama, C., Takahashi, N. and Hirose, M. 2003. Impact of dietary exposure to methoxychlor, genistein, or diisononyl phthalate during the perinatal period on the development of the rat endocrine/reproductive systems in later life. *Toxicology* **192**: 149–170.
11. Mileusnic, D., Lee, J. M., Magnuson, D. J., Hejna, M. J., Krause, J. E., Lorens, J. B. and Lorens, S. A. 1999. Neurokinin-3 receptor distribution in rat and human brain: an immunohistochemical study. *Neuroscience* **89**: 1269–1290.
12. Montero-Pedrazuela, A., Venero, C., Lavado-Autric, R., Fernández-Lamo, I., García-Verdugo, J. M., Bernal, J. and Guadaño-Ferraz, A. 2006. Modulation of adult hippocampal neurogenesis by thyroid hormones: implications in depressive-like behavior. *Mol. Psychiatry* **11**: 361–371.
13. Nakamura, R., Teshima, R., Hachisuka, A., Sato, Y., Takagi, K., Nakamura, R., Woo, G-H., Shibutani, M. and Sawada, J. 2007. Effects of developmental hypothyroidism induced by maternal administration of methimazole or propylthiouracil on the immune system of rats. *Int. Immunopharmacol.* **7**: 1630–1638.
14. Nordquist, R. E., Durkin, S., Jacquet, A. and Spooren, W. 2008. The tachykinin NK3 receptor agonist senktide induces locomotor activity in male Mongolian gerbils. *Eur. J. Pharmacol.* **600**: 87–92.
15. Numachi, Y., Yoshida, S., Yamashita, M., Fujiyama, K., Toda, S., Matsuoka, H., Kajii, Y. and Nishikawa, T. 2007. Altered EphA5 mRNA expression in rat brain with a single methamphetamine treatment. *Neurosci. Lett.* **424**: 116–121.
16. Oh-Nishi, A., Saji, M., Furudate, S. I. and Suzuki, N. 2005. Dopamine D_2-like receptor function is converted from excitatory to inhibitory by thyroxine in the developmental hippocampus. *J. Neuroendocrinol.* **17**: 836–845.
17. Olivieri, G. and Miescher, G. C. 1999. Immunohistochemical localization of EphA5 in the adult human central nervous system. *J. Histochem. Cytochem.* **47**: 855–861.
18. Porterfield, S. P. 2000. Thyroidal dysfunction and environmental chemicals—Potential impact on brain development. *Environ. Health Perspect.* **108**: 433–438.
19. Royland, J. E., Parker, J. S. and Gilbert, M. E. 2008. A genomic analysis of subclinical hypothyroidism in hippocampus and neocortex of the developing rat brain. *J. Neuroendocrinol.* **20**: 1319–1338.
20. Salthun-Lassalle, B., Traver, S., Hirsch, E. C. and Michel, P. P. 2005. Substance P, neurokinins A and B, and synthetic tachykinin peptides protect mesencephalic dopaminergic neurons in culture via an activity-dependent mechanism. *Mol. Pharmacol.* **68**: 1214–1224.
21. Schoonover, C. M., Seibel, M. M., Jolson, D. M., Stack, M. J., Rahman, R. J., Jones, S. A., Mariash, C. N. and Anderson, G. W. 2004 Thyroid hormone regulates oligodendrocyte accumulation in developing rat brain white matter tracts. *Endocrinology* **145**: 5013–5020.
22. Shibutani, M., Uneyama, C., Miyazaki, K., Toyoda, K. and Hirose, M. 2000. Methacarn fixation: a novel tool for analysis of gene expressions in paraffin-embedded tissue specimens. *Lab. Invest.* **80**: 199–208.
23. Shibutani, M., Lee, K-Y., Igarashi, K., Woo, G-H., Inoue, K., Nishimura, T. and Hirose, M. 2007. Hypothalamus region-specific global gene expression profiling in early stages of central endocrine disruption in rat neonates injected with estradiol benzoate or flutamide. *Dev. Neurobiol.* **67**: 253–269.
24. Shibutani, M., Woo, G-H., Fujimoto, H., Saegusa, Y., Takahashi, M., Inoue, K., Hirose, M. and Nishikawa, A. 2009. Assessment of developmental effects of hypothyroidism in rats from in utero and lactation exposure to anti-thyroid agents. *Reprod. Toxicol.* **28**: 297–307.
25. Smith, P. W. and Dawson, L. A. 2008. Neurokinin 3 (NK3) receptor modulators for the treatment of psychiatric disorders. *Recent Pat. CNS Drug Discov.* **3**: 1–15.
26. Takagi, H., Shibutani, M., Kato, N., Fujita, H., Lee, K-Y., Takigami, S., Mitsumori, K. and Hirose, M. 2004. Microdissected region-specific gene expression analysis with methacarn-fixed, paraffin-embedded tissues by real-time RT-PCR. *J. Histochem. Cytochem.* **52**: 903–913.
27. Uneyama, C., Shibutani, M., Masutomi, N., Takagi, H. and Hirose, M. 2002. Methacarn fixation for genomic DNA analysis in microdissected, paraffin-embedded tissue specimens. *J. Histochem. Cytochem.* **50**: 1237–1245.
28. Woo, G-H., Takahashi, M., Inoue, K., Fujimoto, H., Igarashi, K., Kanno, J., Hirose, M., Nishikawa, A. and Shibutani, M. 2009. Cellular distributions of molecules with altered expression specific to thyroid proliferative lesions developing in a rat thyroid carcinogenesis model. *Cancer Sci.* **100**: 617–625.

The Journal of Toxicological Sciences (J. Toxicol. Sci.)
Vol.34, Special Issue II, SP279-SP286, 2009

Intrauterine environment-genome interaction and Children's development (2): Brain structure impairment and behavioral disturbance induced in male mice offspring by a single intraperitoneal administration of domoic acid (DA) to their dams

Kentaro Tanemura, Katsuhide Igarashi, Toshiko-R Matsugami, Ken-ichi Aisaki, Satoshi Kitajima and Jun Kanno

Division of Cellular & Molecular Toxicology, Biological Safety Research Center, National Institute of Health Sciences, 1-18-1 Kamiyoga, Setagaya-ku, Tokyo 158-8501, Japan

(Received February 17, 2009)

ABSTRACT — To demonstrate induction of delayed central nervous toxicity by disturbing neuronal activities in the developing brain, we administered a single intraperitoneal dose of domoic acid (DA; 1 mg/kg), a potent glutamate receptor agonist, to pregnant female mice at the gestational day of 11.5, 14.5 or 17.5. The dams had recovered from acute symptoms within 24 hr, followed by normal delivery, feeding and weaning. All male offspring mice after weaning were apparently normal in response to handlers during cage maintenance, body weight measurement and to mate mice in group housing conditions. At the age of 11 weeks, our neurobehavior testing battery revealed severe impairment of learning and memory with serious deviances of anxiety-related behaviors. The developed brain of prenatally exposed mice showed myelination failure and the overgrowth of neuronal processes of the limbic cortex neurons. This study indicates that the temporal disturbance of neurotransmission of the developing brain induces irreversible structural and functional damage to offspring which becomes monitorable in their adulthood by a proper battery of neurobehavioral tests.

Key words: Domoic acid, Prenatal exposure, Brain structure, Behavior

INTRODUCTION

Adequate neural activities are necessary for the maturation of neural networks during brain development (Rice and Barone, 2000). Historically, the presence of such plasticity-driven mechanisms has been demonstrated by a series of studies of eyelid suture in kittens or monkeys and corresponding findings reported in young human cataracta patients (Wiesel, 1982; Gu *et al.*, 1989; Fonta *et al.*, 2000). These processes require proper stimuli to the brain that trigger the release of neurotransmitters from the neurons and subsequent receptor-mediated signal transduction (Ooi and Wood, 2008; Greer and Greenberg, 2008; Cohen-Cory, 2002). Therefore, it is highly conceivable that disturbance of neural activities by neuroactive xenobiotics leads to malformation of the fine structure of the brain. Even when the exposure was transient, it would result in anomaly of higher brain functions in adulthood without overt signs of brain damage during maturation.

Glutamate receptors begin to express in the late embryonic stages, and their expression increases with the advance of brain development (Luján *et al.*, 2005; Manent *et al.*, 2005). Prenatal exposure of xenobiotic chemicals that interfere with the glutamate receptor function could induce malformation of the fine structure of the brain which should lead to anomaly of higher brain function that is different from acute neurotoxicity known for such chemicals to induce in adults (Bondy and Campbell, 2005). A marine biotoxin domoic acid (DA) which is structurally related to glutamate, and activates ionotropic α-amino-3-hydroxy-5-methyl-4-isoxazolepropionic acid (AMPA) and kinate subtypes of glutamate receptors (Pulido, 2008) is known to cause acute symptoms of diarrhea, seizures and memory loss in adult human by eating contaminated shellfish (Tryphonas and Iverson, 1990), and DA induced acute neurotoxicity in animal

Correspondence: Jun Kanno (E-mail: kanno@nihs.go.jp)

model (Chandrasekaran *et al.*, 2004). Additionally, DA is also known to cross the placenta, and enters prenatal brain tissue in rats (Maucher and Ramsdell, 2007). Therefore, prenatal exposure of DA may disrupt the neural activities by excessive stimulation of glutamate receptors, and should induce fine structural and functional disorganization in the developing brain. Here, we report that a transient transplacental DA exposure *in utero* induced alteration of the neurobehavioral parameters and corresponding fine brain structure of the male C57BL/6 mice in their adulthood.

MATERIALS AND METHODS

Animal treatment

All experiments were carried out under approval of Experimental Animal Use Committee of National Institute of Health Sciences, Japan. Pregnant C57LB/6 female mice obtained from Japan SLC, Inc., were individually housed in plastic breeding cages with free access to water and pellet diet (CRF-1; Oriental Yeast Co., Tokyo, Japan) in a 12 hr light-dark cycle conventional condition. Four groups with five pregnant mice each were prepared. All groups received three intraperitoneal injections on gestational day 11.5 (E11.5) as a late embryonic period, 14.5 (E14.5) and 17.5 (E17.5) as early and late fetal period respectively. Group A (Control) received three i.p. shots of saline on E11.5, E14.5 and E17.5. Group B (DA@ E11.5) received one shot of DA (Calbiochem, San Diego, CA, USA) at a dosage of 1 mg/kg on E 11.5 and two shots of saline on E14.5 and E17.5. Group C (DA@14.5) received a shot of saline on E11.5, a shot of DA on E14.5 and another saline on E17.5. Group D (DA@E17.5) received two shots of saline on E11.5 and E14.5 , and a shot of DA on E17.5. The pups were weaned at 4 weeks of age, and four male mice per liter were randomly selected and housed in one cage with free access to water and CRF-1 pellet until 11 weeks of age.

Immunohistochemical analysis

Brains (n = 4 male mice per group) were fixed with methacarn fixative (methanol: chloroform:acetic acid, 60:30:10 v/v) and paraffin-embedded sections were prepared. Mouse monoclonal anti-microtubule associated protein 2 (MAP2, sc-32791; Santa Cruz, CA, USA), mouse monoclonal anti-neurofilament-m (NF-M, sc-20013; Santa Cruz, CA, USA), rabbit polyclonal anti-myelin associated glycoprotein (MAG, sc-15324; Santa Cruz, CA, USA), and rabbit polyclonal anti MAP2 (sc-20172; Santa Cruz, CA, USA) were used. Deparaffinized sections were pretreated with HistoVT-One (Nacalai Tesque, Kyoto, Japan.) as previously described (Tanemura *et al.*, 2005) and incubated with primary antibodies. Secondary antibodies were Alexa 568-conjugated anti-mouse IgG and Alexa 488-conjugated anti-rabbit IgG (Molecular Probes, Eugene, OR, USA). Fluorescent images were obtained with an FV-300 confocal laser scanning microscope (Olympus, Tokyo, Japan). For semi-quantitative analysis of images, we calculated the ratio of fluorescence intensity compared to control mice (group A), by using the IMAGE J program (http://rsb.info.nih.gov/ij/index.html. National Institute of Health, Bethesda), after adjusting background noise (n = 4 images per mouse).

Neurobehavioral tests

A battery of neurobehavioral tests were conducted on open field test (OF), light/dark transition test (LD), elevated plus maze test (EP) and contextual/cued fear conditioning test (FZ). Experimental apparatuses and image analyzing softwares were obtained from O'Hara & Co., Ltd., Japan. Image analyzing softwares (Image OF4, Image LD2, Image EP2 and Image FZ2) were developed from the public domain IMAGE J program. All experiments were done with 8 mice per group (32 mice total), and were conducted between 13:30 and 16:30. The level of background noise during behavioural testing was about 50 dBA. After each trial, the apparatuses were wiped and cleaned.

Open field test

The locomotor activity was measured for 10 min using an open field apparatus made of white plastic (50 x 50 x 40 (H) cm).

An LED light system was positioned 50 cm above the centre of the field (50 lux at the centre of field). Total distance travelled (cm), time spent in the central area (30% of the field) (sec), and the frequencies of movement were measured (Tanemura *et al.*, 2002).

Light/dark transition test

The apparatus used for the light/dark transition test consisted of a cage (21 x 42 x 25(H) cm) divided into two chambers by a partition with an opening. One chamber is brightly illuminated (250 lux), whereas the other chamber is dark (2 lux). A mouse is placed into the dark area and allowed to move freely between the two chambers through the opening for 5 min. The latency for the first move to the light area, the total number of transitions and the time spent on each side were measured.

Elevated plus maze test

The plus-shaped apparatus consisted of four arms (25

x 5 cm) connected to a central square area (5 x 5 cm). Opposite two arms are enclosed with 20 cm-high transparent walls and other two are left open. The floor of the maze is made of white plastic plate and is elevated 60 cm above the room floor (200 lux at the centre of the apparatus). A mouse is placed to the central square area of the maze, facing one of the open arms, and the behavior was recorded for 10 min: total distance traveled (cm), total time on open arms and central square area (sec) and the total number of entry to any of the arms (Tanemura *et al.*, 2002).

Contextual/cued fear conditioning test

The apparatus consists of a conditioning chamber (or a test chamber) (17 x 10 x 10 (H) cm) made of clear plastic with ceiling and placed in a sound proof box. The chamber floor has stainless steel rods (2-mm diameter) spaced 5 mm apart for giving electric foot shock (0.1 mA, 3 sec duration) to the mouse. The soundproof box consists of white-coloured wood, and is equipped with an audio speaker and light source (35 lux at the centre of the floor). A CCD camera is positioned 20 cm above the ceiling of the chamber. During the conditioning trial (Day 1), mice are placed individually into the conditioning chamber in the sound proof box and, after 90 sec, they are given three tone-shock pairings (30 sec of tone, 75 dB, 10 KHz followed by 3 sec of electric shock at the end of tone, 0.1 mA) separated by 90 sec. Then they are returned to their home cage. Next day (Day 2), as a "contextual fear test", they are returned to the conditioning chamber without tone and shock for a 6-min. On the third day (Day 3), they are brought to a novel chamber of different make without stainless steel rods place in the sound proof box and, after a period of 3 min, only the conditioning tone is presented for 3 min (no shock was presented, 35 lux at the centre of the floor). The freezing response of mice was defined as a consecutive 2 sec period of immobility. Freezing rate (%) was calculated as [time freezing/session time] x 100 (Tatebayashi *et al.*, 2002).

Statistical analysis

Data were indicated as means ± S.D. Statistical analysis was conducted with student's t-test by using StatView (SAS Institute, Cary, NC, USA). A p-value of < 0.05 compared to the results of control male mice (group A) was considered statistically significant.

RESULTS

Effects on morphology of brain by prenatal exposure to DA

Offspring mice of all groups after weaning up to the age of 11 weeks were apparently normal in response to handlers during cage maintenance, body weight measurement and to mate mice in group housing conditions. Routine histological observation of the brain at 11 weeks old by hematoxylin-eosin staining could not reveal difference among the groups (data not shown). By immunohistochemical study on the same brain sections, reduced immuno-reactivity against the MAG, the marker for myelin, was detected in the cortices of group B (DA@11.5) and C (DA@14.5) compared to control (Figs. 1A-D and I). In contrast, increased immuno-reactivity against MAP2, the marker for neuronal dendrite, was indicated in the same area of group B (DA@11.5), C (DA@14.5) and D (DA@17.5) compared to control (Figs. 1E-H and J). Increased immuno-reactivity against MAP2 was also found in lateral area of CA3 hippocampus of group B (DA@11.5), C (DA@14.5) and D (DA@17.5) compared to control, whereas immuno-reactivity for MAP2 showed no significant difference in medial area of CA3 hippocampus among the groups (Figs. 2A-D and I). Immuno-reactivity against NF-M; the marker for neuronal axon, also showed no significant difference in the same area among the groups (Figs. 2E-H and J).

Effects on behavior by prenatal exposure of DA

In the OF test, the distance traveled was not different among the groups (Fig. 3A), the time spent in center area was significantly prolonged in group D (DA@17.5) mice (Fig. 3B). In the LD test, group C (DA@14.5) mice stayed in light area for longer time (Fig. 4A), and latency for the first move to light area was significantly shorter in group C (DA@14.5) and D (DA@17.5) (Fig. 4B). In the EP test, significantly increased distance traveled and time spent in the open area were detected for group B (DA@11.5), C (DA@14.5) and D (DA@17.5) (Figs. 5A and B). In the FZ test, both Day 1 and Day 2 freezing responses of group C (DA@14.5) and D (DA@17.5) were significantly reduced compared to control (Figs. 6A and B).

DISCUSSION

The expression levels of glutamate receptors starts to elevate at the fetal period, i.e. approximately from E14 (Luján *et al.*, 2005; Manent *et al.*, 2005). Exogenous glutamatergic stimuli at this period would affect the for-

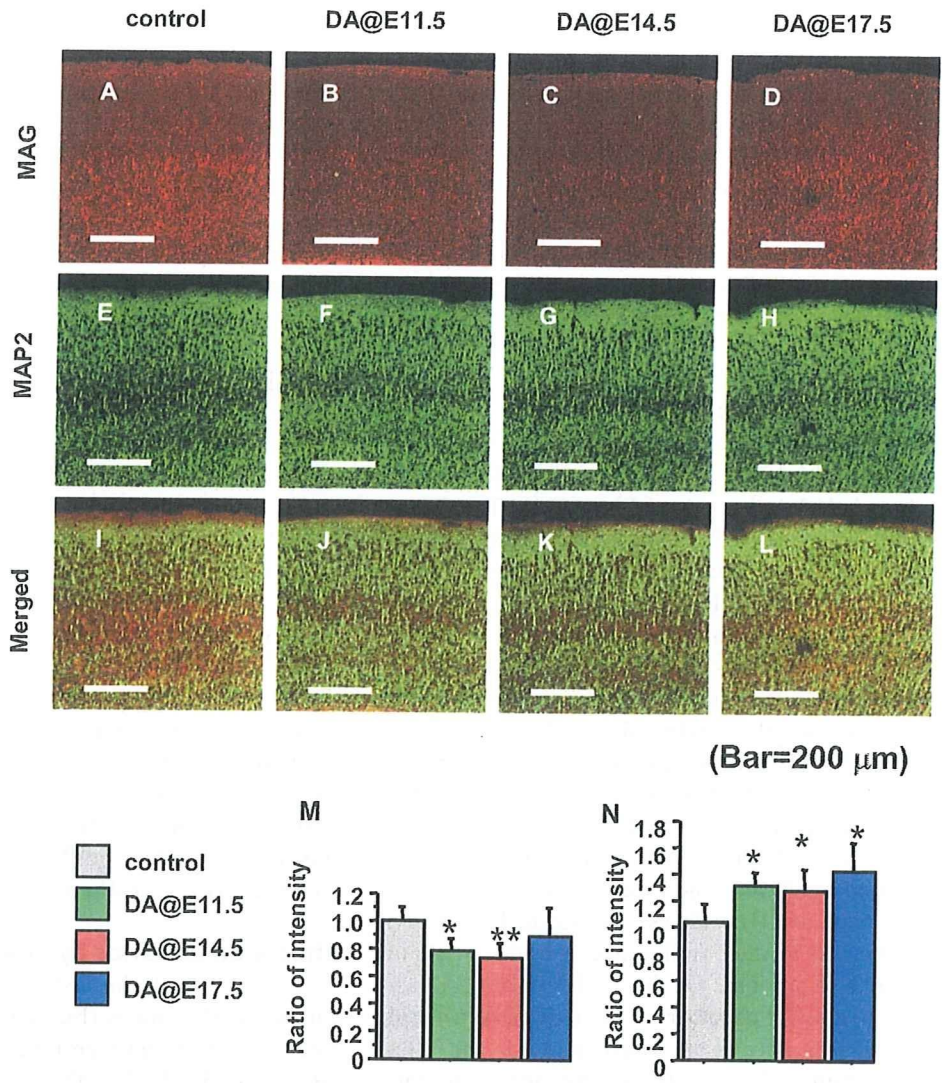

Fig. 1. Delayed effects on cerebral cortex induced by prenatal exposure of DA.
A-D, Immunohistochemical staining against MAG; E-H, immunohistochamical staining against MAP2; I-L, merged images of the cerebral cortex. A, E, I, group A (control), B, F, J, group B (DA@11.5), C, G, K, group C (DA@14.5) and D, H, L, group D (DA@17.5). Scale bar = 200 mm. M, Quantitative analysis in intensity ratio to control of MAG expression, and J, MAP2 expression among the groups (mean ± S.E.M.). Asterisk (**) and (*) indicate significant difference compared to control ($P < 0.01$) and ($P < 0.05$).

mation of the neural circuits. An extreme example to support this hypothesis would be the phenotype of the double knockout mouse of glutamate transportors GLT1 and GLAST (Matsugami *et al.*, 2006). Lack of these transportors is considered to result in abnormally high concentration of glutamate in the brain. In fact, morphological anomaly became apparent in synchronization with the expression of glutamine receptors. In our study, corresponding to the hypothesis, the neurobehavioral symptoms as a whole was severer for those exposed at fetal periods, i.e. E14.5 and E17.5, compared to those at embryonic period, i.e. E11.5 (Fig. 7).

We demonstrated that a prenatal exposure of a relatively low dose of DA induced a spectrum of neurobehavioral anomalies which became monitorable at the adult stage accompanied by alteration in fine brain structures detectable by immunohistochemistry. It is emphasized that this amount of DA did not induce abnormal responses dur-